frontiers | Frontiers in Marine Science

TYPE Original Research
PUBLISHED 26 March 2025
DOI 10.3389/fmars.2025.1554418

OPEN ACCESS

EDITED BY
Hajime Kayanne,
The University of Tokyo, Japan

REVIEWED BY
Moyang Li,
Xiamen University, China
Atsuko Yamazaki,
Nagoya University, Japan

*CORRESPONDENCE
Daniel M. Sigman
sigman@princeton.edu

RECEIVED 02 January 2025
ACCEPTED 24 February 2025
PUBLISHED 26 March 2025

CITATION
Luu VH, Ryu Y, Darling WS, Oleynik S, de Putron SJ, Cohen AL, Wang XT and Sigman DM (2025) Nitrogen isotope ratios across the Bermuda coral reef: implications for coral nitrogen sources and the coral-bound nitrogen isotope proxy. *Front. Mar. Sci.* 12:1554418. doi: 10.3389/fmars.2025.1554418

Nitrogen isotope ratios across the Bermuda coral reef: implications for coral nitrogen sources and the coral-bound nitrogen isotope proxy

Victoria H. Luu[1], Yeongjun Ryu[1], Wren S. Darling[1], Sergey Oleynik[1], Samantha J. de Putron[2], Anne L. Cohen[3], Xingchen Tony Wang[4] and Daniel M. Sigman[1]*

[1]Department of Geosciences, Princeton University, Princeton, NJ, United States, [2]Bermuda Institute of Ocean Sciences, St. George's, Bermuda, [3]Department of Geology and Geophysics, Woods Hole Oceanographic Institution, Woods Hole, MA, United States, [4]Department of Earth and Environmental Sciences, Boston College, Chestnut Hill, MA, United States

The nitrogen (N) isotopic composition of coral tissue provides insight into N sources and cycling on reefs, and coral skeleton-bound organic matter (CS-δ^{15}N) can extend these insights into the past. Across the Bermuda platform, we measured the δ^{15}N of four coral species and their potential N sources, as well as an asymbiotic filter feeder as a comparative heterotroph and benthic macroalgae as a comparative autotroph. Organisms and organic N pools from the coral reefs exhibit a δ^{15}N increase toward the Bermuda coast, likely due to anthropogenic N inputs. At all sites, the δ^{15}N of bulk coral tissue is consistent with corals feeding dominantly on zooplankton-sized organic matter and some smaller suspended particulate N. The corals lack the trophic δ^{15}N elevation that characterizes serpulids; this is consistent with internal recycling and retention of low-δ^{15}N metabolic N by symbiont-bearing corals. The data are inconsistent with corals' reliance on the dissolved inorganic N used by macroalgae at the same sites. Among coral species, two species with smaller polyps (1-2 mm) have ~1‰ lower bulk tissue δ^{15}N than two counterparts with larger polyps (5-10 mm), perhaps due to differences in food source. Taxon-specific δ^{15}N differences are also observed between coral tissue and skeleton-bound N, with larger differences in the two small-polyp species. In net, however, CS-δ^{15}N mean values and spatial gradients were similar in the four species studied.

KEYWORDS

coral, nitrogen, stable isotope, coral skeleton, Bermuda, food web

1 Introduction

Since ~240 million years ago, scleractinian corals have evolved to become the dominant builders of reef systems and are widespread in modern day tropical and subtropical coastal oceans (Stanley, 1981). These stony corals can be long-lived (hundreds of years) and have a relatively fast growth rate (0.3-2.0 cm/year) (Piper, 2007), recording the chemistry of their environment as they secrete their calcium carbonate skeleton. As such, coral skeleton has been pursued as a proxy for high-resolution reconstructions in studies of climate variability and past ocean chemistry, beginning with applications involving the inorganic and structural components of coral skeleton (Druffel, 1997; Corrège, 2006). Reconstructions utilizing the nitrogen (N) in organic matter bound within the skeleton, which constitutes less than 0.1% of the skeletal material by weight (Muscatine et al., 2005; Wang et al., 2015; Erler et al., 2016), is a more recent focus. The $^{15}N/^{14}N$ ratio (or "$\delta^{15}N$") of this coral skeleton-bound organic matter (CS-$\delta^{15}N$) has been suggested as a proxy for the $\delta^{15}N$ of the corals' N source and thus of the fixed N in the environment (Hoegh-Gulberg, 2004; Muscatine et al., 2005) ($\delta^{15}N = ((^{15}N/^{14}N)_{sample})/(^{15}N/^{14}N)_{reference} - 1)*1000$, where atmospheric N_2 is the universal reference). CS-$\delta^{15}N$ has since been applied to track spatial and temporal changes in water column $\delta^{15}N$, which can provide insight to past and present N cycling dynamics (e.g., Marion et al., 2005; Yamazaki et al., 2011a, 2011b; Erler et al., 2016; Ren et al., 2017; Wang et al., 2018; Duprey et al., 2020; Erler et al., 2020). With the development of more sensitive methods, it has become practical to ground-truth the relationship between CS-$\delta^{15}N$ and environmental N $\delta^{15}N$ through modern field studies (e.g., Choisnard et al., 2024; Erler et al., 2015; Wang et al., 2015, 2016; Rangel et al., 2019). However, such work must contend with the complexity of reef organisms and ecosystems, and many fundamental questions remain.

Whether the interest is in CS-$\delta^{15}N$ as a tool for paleoenvironmental reconstruction or simply in understanding the environmental sensitivities of corals, a central question is their source of nutrition. Within their tissues, shallow scleractinian corals often harbor photosynthetic endosymbionts, commonly referred to as zooxanthellae. A portion of the photosynthate from the endosymbionts ultimately flows to the coral host (Wilkerson and Trench, 1986; Muscatine et al., 2005), whether by a specific transfer mechanism (Tanaka et al., 2006) or by the host coral feeding on the symbionts (Wiedenmann et al., 2023). Laboratory experiments have shown that corals' symbionts are capable of assimilating dissolved inorganic N (DIN; e.g., ammonium and nitrate) from the environment (Grover et al., 2002, 2003; Pernice et al., 2012). This ability has led to the proposal that the coral system relies on inorganic nutrient uptake by the symbionts, which then photosynthesize and produce organic matter for the coral system (Wiedenmann et al., 2023). Yet, the coral itself is a heterotrophic organism that is equipped with tentacles and cellular machinery for the capture and intake of prey, including nematocyst stinging cells, and the collection of particulate organic matter (POM) in general (e.g., Szmant-Froelich and Pilson, 1984; Ferrier-Pagès et al., 2003, 2010). Given the limited availability of DIN in nutrient-poor tropical and subtropical reefs, it would seem reasonable to expect that host feeding accounts for most of a coral system's N intake. Indeed, one can argue that it is the excess N (and phosphorus) that results from feeding and host metabolism that underpins the success of stony scleractinian corals and their symbionts in nutrient-poor tropical and subtropical surface waters (Goreau et al., 1971; Houlbrèque et al., 2004; Houlbrèque and Ferrier-Pagès, 2009; Gustafsson et al., 2013). Whether corals rely on feeding or DIN assimilation for N acquisition, host-symbiont N recycling has implications for the $\delta^{15}N$ of the coral's tissue and skeleton. In particular, it can reduce the trophic $\delta^{15}N$ elevation that is observed in most heterotrophs, and possibly to variable degrees (Erler et al., 2015; Wang et al., 2015). Moreover, with these diverse options to meet corals' energetic and anabolic needs, tank experiments on corals may not be representative of what forms of N corals rely on in the natural environment. As a result, there is a need for further field studies to examine how coral $\delta^{15}N$ relates to the $\delta^{15}N$ of environmental fixed N and what these relationships indicate about coral N nutrition and the environmental and biotic signals that CS-$\delta^{15}N$ records.

Wang et al. (2015) found that CS-$\delta^{15}N$ exhibited a gradient across the Bermuda platform, and Baker et al. (2017) observed a similar gradient in the $\delta^{15}N$ of the proteinaceous skeletons of soft corals. Baker et al. argued that the gradient could be explained by a gradient in the $\delta^{15}N$ of DIN that was caused by anthropogenic inputs from Bermuda's sewage-influenced groundwater lens, sewage outfalls, and tourism infrastructure. Indeed, Sims et al. (2020) identified and studied one site of groundwater DIN discharge along the island's rocky shore, measuring high nitrate concentrations and elevated nitrate $\delta^{15}N$, which was reflected in the $\delta^{15}N$ of benthic macroalgae and coral tissue near the site of discharge.

Here, we expand upon these studies of the Bermuda platform, taking advantage of this previously identified inshore-offshore N isotopic gradient as an environmental signal, even if of uncertain origin. For five sites extending from nearshore to the edge of the platform (Figure 1), we report measurements of the $\delta^{15}N$ of (1)

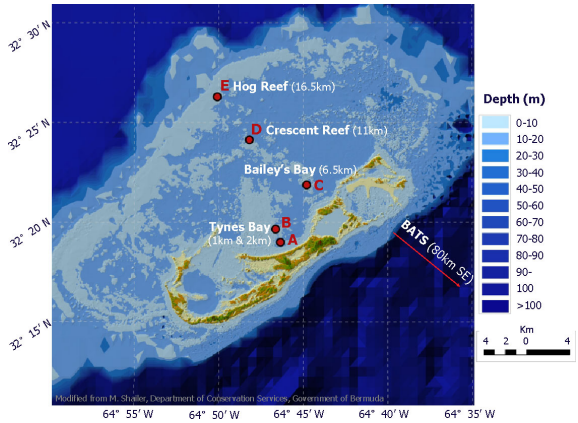

FIGURE 1
Map of reef study sites across the Bermuda platform. Map credit: M. Shailer, Department of Conservation Services, Government of Bermuda.

corals, their symbionts, and their skeletons, (2) several of corals' possible N sources, and (3) organisms with which comparison is informative. Our goal is to illuminate both the place of corals in the Bermuda reef ecosystem and the signals recorded by CS-δ^{15}N.

2 Materials and methods

2.1 Field sampling

Five sampling locations spanned from just north of the island to the north rim of the Bermuda platform: Tynes Bay (A, 1 km), Tynes Bay (B, 2 km), Bailey's Bay Reef Flats (C), Crescent Reef (D), and Hog Reef (E) (Figure 1). A small boat (Twin Vee) of the Bermuda Institute of Ocean Sciences (BIOS) was taken into the field for five consecutive days of sampling in June 2017.

At each site, acid-washed HDPE carboys were used to collect 20 L of surface water for PN samples. Between each sampling, carboys were rinsed three times with water from the site prior to sample collection. The collected seawater was filtered across a 47 mm glass fiber filter (Advantec GF75; 0.3 μm pore size; pre-combusted at 450°C for 4 hours) using a low-flow peristaltic pump (Masterflex L/S® Portable Sampling Pump). The filters were loosely covered in pre-combusted aluminum foil, placed inside petri dishes, sealed with electrical tape, and stored on ice in a cooler until transferred to a –80°C freezer at the end of the sampling shift. Additional on-platform PN samples were collected in a similar fashion in 2014 at sites D and E. Aliquots of the filtered seawater were collected in 150 mL acid-washed HDPE bottles after triple-rinsing with sample water, sealed, and stored on ice in a cooler until transferred to a –20°C freezer at the end of the sampling shift.

Plankton net tows were conducted at each site by towing a plankton net (mesh size 35 μm) just beneath the surface for 10 minutes at low speed. An aliquot was reserved as a bulk total sample, and the rest was sequentially filtered through mesh screens to collect subsamples along the size distributions of 35-250 μm, 250-500 μm, and 500-1000 μm. All net tow samples were transferred to acid-washed HDPE bottles and stored on ice in a cooler. Upon returning to the laboratory, the net tow samples were collected onto pre-combusted glass fiber filters, which were sealed in petri dishes as described above and stored in a –80°C freezer.

After the water column sampling at each site was complete, the boat was anchored, and divers collected coral, macroalgae, and serpulid worms by hand via SCUBA. All samples were collected from between 3 m and 9 m depth. We studied four species of mounding corals with different morphologies and coral polyp sizes: *Porites astreoides* (1-2 mm polyps), *Madracis decactis* (1-2 mm polyps), *Diploria labyrinthiformis* (5-10 mm polyps), and *Montastrea cavernosa* (5-10 mm polyps). At each site, coral fragments with approximately 4 cm by 4 cm of soft tissue area and 4 cm of skeleton were chiseled from three separate colonies for each species. Three types of benthic macroalgae were collected: *Caulerpa* sp., *Laurencia* sp., and *Dictyota* sp. At each site, at least three samples of each genus were collected if present. At least three samples of serpulid worms (family *Serpulidae*, here after serpulids) were collected at each site, collected by harvesting pieces of hydrozoan fire coral (*Millepora alcicornis*) around which the worms built their tubes. All samples were kept in coolers filled with local seawater for a short amount of time. Upon return to the laboratory, all specimens were processed and subsequently stored in a –80°C freezer. Corals and macroalgae were wrapped with pre-combusted aluminum foil and placed into plastic bags. The serpulid worms were removed from their tubes prior to packaging. Samples were transported frozen to Princeton University, Princeton, NJ and stored in –80°C (organic samples) or –20°C (water samples) freezers until analysis.

2.2 Sample analysis

2.2.1 Soft tissue

Macroalgae, serpulid worm, and plankton net tow samples were freeze-dried (Labconco FreeZone 2.5; 0.315 Torr, –54°C), ground to fine powder, weighed out, and packed into tin capsules for measurement by combustion coupled with isotope ratio mass spectrometry (Elementar Vario Isotope Cube elemental analyzer to Elementar Isoprime visION). PN samples and their glass fiber filter carrier were freeze-dried and packed into tin capsules. PN samples from 2014, 2017, and 2019 were portioned using a metal corer with known diameter in order to calculate PN concentrations as well.

Coral samples were thawed at room temperature, and tissue was removed from the skeleton using an air pick. The coral bulk tissue was suspended in filtered low-nutrient seawater, homogenized using a Wheaton glass Tenbroeck tissue grinder, and transferred to an acid-washed 15 mL centrifuge tube. An aliquot of the homogenized sample was reserved for the measurement of bulk tissue N isotopes. The remainder of the homogenized sample was separated into coral animal tissue and zooxanthellae portions via centrifugation (with minor modifications from Muscatine et al., 1989). The animal tissue portion was centrifuged three times (10000 RCF), transferring tubes each time, to remove zooxanthellae. The zooxanthellae portion was centrifuged at least three times (1500 RCF, sufficient to just pellet the zooxanthellae and leave residual coral tissue in suspension), discarding the supernatant and resuspending the pellet in filtered low-nutrient seawater each time to remove traces of host tissue. The processed samples were immediately stored in a –20°C freezer and later transferred into a –80°C freezer. The coral bulk tissue, host tissue, and symbiont samples were all freeze dried and prepared for measurement as described above.

All samples were analyzed in duplicate when enough material was available and were calibrated against an in-house aminocaproic acid isotopic standard and an international glutamic acid isotopic reference (USGS40). The analytical precision (1 SD) was <0.1‰.

2.2.2 Coral skeleton

After removal of the soft tissue, a Dremel tool was used to subsample a coral piece within the upper 1-2 cm of the coral skeleton. Each of these pieces underwent a preliminary oxidative cleaning with sodium hypochlorite (reagent grade, 10-15%) for 24 h in a 15 mL polypropylene centrifuge tube, after which they were

rinsed thoroughly with MilliQ deionized water and dried at 60°C. To ensure that the entire tissue-occupied region of skeleton would be included while minimizing contribution from older skeleton, the top 0.5 cm for *P. astreoides* and *M. decactis* samples and the top 1 cm for *D. labyrinthiformis* and *M. cavernosa* samples were subsampled using a Dremel tool. Although a more precise method for this type of soft tissue-to-skeleton comparison would be to stain the colony at the time of soft tissue collection and return at a later date for collection of the skeleton, this would be difficult for the needed sample quantity. The approaches used here should be sufficient for investigating the typical relationship between coral soft tissue and the organic matrix preserved within the coral skeleton across multiple sites.

The subsampled, pre-cleaned skeletal fragments were ground to <250 μm using a mortar and pestle. 10-15 mg of the coral powder per sample was aliquoted into 15 mL polypropylene centrifuge tubes and underwent a second oxidative cleaning with sodium hypochlorite for 24 h, rinsed three times with MilliQ deionized water, and dried at 60°C (Wang et al., 2015). The powdered coral samples were weighed into pre-combusted 4 mL glass vials and dissolved into 4N HCl (Optima Grade) to release the organic matrix, which was then quantitatively oxidized to nitrate using a 1 mL aliquot of freshly combined persulfate oxidizing reagent (1 g recrystallized low-N potassium potassium persulfate and 2 g ACS grade NaOH in 100 mL deionized, distilled water) at 120°C in an autoclave. After oxidation, the sample was centrifuged, and the supernatant was transferred to a new pre-combusted 4 mL glass vial and pH-adjusted to neutral using 4N HCl. The nitrate concentration of the sample solution was analyzed by chemiluminescence (Braman and Hendrix, 1989) to determine aliquot volumes for $\delta^{15}N$ measurement. The $\delta^{15}N$ of the nitrate was then measured by quantitative conversion to N_2O with the "denitrifier method" (Sigman et al., 2001) followed by automated extraction, purification, and isotopic analysis of the N_2O product by isotope ratio mass spectrometry (IRMS; Thermo MAT 253; Casciotti et al., 2002; McIlvin and Casciotti, 2011; Weigand et al., 2016). Amino acid isotopic reference materials USGS 40 and 41 were used in each batch of analyses to correct for the reagent and operational blanks, which was less than 5% of the total N content in any oxidized sample. The analytical precision (1 SD) of the total protocol was <0.2‰.

2.2.3 Water samples

Ammonium concentration was measured fluorometrically (modified from Holmes et al., 1999). A 2 mL aliquot of working reagent (4 g ortho-phthaldialdehyde in 100 mL ethanol, with 0.8 g sodium sulfite and 80 g sodium borate in 2 L deionized water) was added to a 2 mL aliquot of sample seawater in 4 mL pre-combusted glass vials, left to incubate in the dark for 2 h, and then read on a fluorometer (Turner Designs Trilogy Laboratory Fluorometer with ammonium module). Total nitrate and nitrite concentration was measured by chemiluminescence (Braman and Hendrix, 1989): sample was aliquoted into a heated chamber of vanadyl sulfate solution to quantitatively reduce nitrate and nitrite to nitric oxide gas, which was transferred by a continuous argon flow to a Teledyne NO_x Analyzer. Appropriate concentration standards were used to generate calibration curves for each method.

3 Results

3.1 $\delta^{15}N$ of organic pools across the Bermuda platform

The N pools were classified into four groups for comparison: autotrophs (i.e., macroalgae and PN), heterotrophs (i.e., serpulid worms and zooplankton net tows), corals with small polyps (i.e., *P. astreoides* and *M. decactis*), and corals with large polyps (i.e., *D. labyrinthiformis* and *M. cavernosa*) (Figure 2).

On average across the entire platform (Figure 2) and typically at each individual site (Table 1), the autotroph pools had the lowest $\delta^{15}N$, and the heterotroph pools had the highest $\delta^{15}N$, with a 2-3‰ offset between the two groups. Among autotrophs, the macroalgae pool had a larger range in $\delta^{15}N$ (~4.5‰) across the pedestal than did PN (~3‰); this was driven primarily by high macroalgae $\delta^{15}N$ at the site nearest to the island (Figures 2, 3). Among heterotrophs, the range in $\delta^{15}N$ was larger for net tows than for serpulid worms (~3.3‰ *vs.* ~2.4‰), also driven in large part by high $\delta^{15}N$ near the island. Coral bulk tissue $\delta^{15}N$ was always higher than the autotrophs and typically slightly lower than the heterotrophs. Coral $\delta^{15}N$ tended to be closer to the heterotrophs than to the autotrophs, particularly for corals with large polyps (Figure 2).

Site average $\delta^{15}N$ for all sample types decreased across the Bermuda platform from nearshore to the north rim (Figures 3, 4). A similar $\delta^{15}N$ gradient was observed by Wang et al. (2015), suggesting that this is a persistent feature of the platform.

3.1.1 Coral $\delta^{15}N$

The coral bulk tissue (i.e., host tissue with symbionts removed from the skeleton) is considered to be representative of the soft tissue of the living coral system as it exists in the natural environment. For corals with large polyps (5-10 mm), bulk tissue $\delta^{15}N$ was similar to the heterotrophs, on average less than 1‰ lower. The bulk tissue $\delta^{15}N$ of corals with small polyps (1-2 mm) was typically slightly (<1‰) lower than corals with large polyps and thus 1-2‰ lower than heterotrophs (Figure 2; Table 1).

In general, the $\delta^{15}N$ for all measured coral components (i.e., bulk tissue, coral host component, coral symbiont component, and coral skeleton-bound organic matter) follow a similar trend across the platform, decreasing from nearshore to offshore (Figure 4). For all four species of corals examined, the $\delta^{15}N$ of soft tissue components decreased by about 2-3‰ across the platform from nearshore to the north rim (Figure 4; Table 1). Small-polyp coral *P. astreoides* (1-2 mm) bulk tissue $\delta^{15}N$ decreased by about 2.5‰ from nearshore to the outermost reef at the north rim (Figure 4a; Table 1), and *M. decactis* (1-2 mm) bulk tissue $\delta^{15}N$ decreased similarly across the same transect (Figure 4b; Table 1). *D. labyrinthiformis*, a coral with large polyps (5-10 mm), had the highest coral bulk tissue $\delta^{15}N$, similar to the $\delta^{15}N$ of serpulid worms and net tow zooplankton, and decreased by just under 3‰ from nearshore to the north rim (Figure 4c; Table 1). *M. cavernosa*, another coral with large polyps (5-10 mm), had coral bulk tissue $\delta^{15}N$ similar to *D. labyrinthiformis* at the three sites farthest from the island, but was instead more similar to *P. astreoides* and *M.*

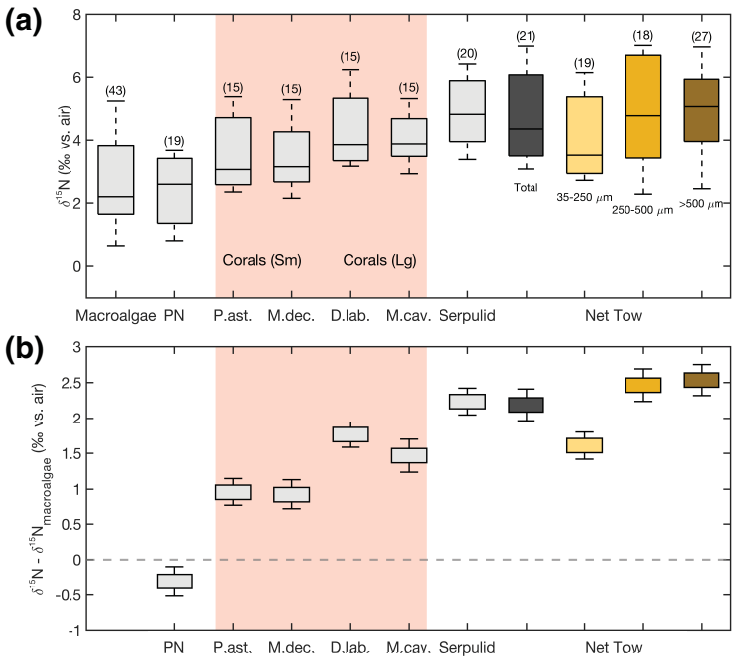

FIGURE 2
(a) Soft tissue $\delta^{15}N$ for samples from all reef sites across the platform. **(b)** The $\delta^{15}N$ differences between these groups and macroalgae $\delta^{15}N$ values. In **(a)**, each box plot shows the 25th and 75th percentiles (box edges), with the interquartile range as the distance between them, and the thick black line indicating the median. Error bars in **(b)** represent the standard error, in order to clarify which differences are statistically significant. While the left-to-right ordering is intended to evoke the $\delta^{15}N$ increase associated with heterotrophy, the net tow size fraction of 35-250 μm could contain large phytoplankton. Pink shading contains the coral data.

decactis at the two sites nearest to the island, resulting in a $\delta^{15}N$ decrease of just under 2‰ from nearshore to the north rim (Figure 4d; Table 1).

The symbiont-to-host $\delta^{15}N$ difference varies across the four species investigated but is relatively stable across sites for each species (Figure 4). The two coral species with smaller polyps, *P. astreoides* and *M. decactis*, are characterized by symbiont $\delta^{15}N$ values that are higher than or similar to the host tissue, while the two coral species with larger polyps have symbiont $\delta^{15}N$ values that are lower than the host tissue. In general, the data conform with the mass-balance expectation that symbiont and host tissue $\delta^{15}N$ should bracket the bulk tissue $\delta^{15}N$. Exceptions imply limitations in existing symbiont-host separation methods, the effects of which may differ between coral species.

P. astreoides CS-$\delta^{15}N$ decreased by just under 3‰ from nearshore to the outermost reef at the north rim (Figure 4a; Table 1). *M. decactis* CS-$\delta^{15}N$ decreased by 2.2‰ across that same transect (Figure 4b; Table 1). *D. labyrinthiformis* decreased by just under 2.5‰ from nearshore to the outermost reef at the north rim (Figure 4c; Table 1). *M. cavernosa* CS-$\delta^{15}N$ decreased only about 1.2‰ across that same transect (Figure 4d; Table 1).

3.1.2 Water column N pools

DIN concentrations were low across the platform, though higher than typical offshore concentrations in the subtropical gyre. Ammonium concentrations were highest near the island (0.25 ± 0.08 μM) and lowest at the north rim (0.07 ± 0.03 μM) (Figure 3c; Table 2). Nitrate+nitrite concentrations averaged 0.29 ± 0.14 μM.

The site average $\delta^{15}N$ of PN decreased across the platform from about 3.5‰ nearshore to 1‰ at the north rim in 2017 (Figure 3a; Table 1). PN concentration decreased by more than half across the platform, from 0.80 ± 0.03 μM of seawater (units hereafter listed as μmol L^{-1}) nearshore to 0.32 ± 0.02 μM at the north rim (Figure 3c; Table 2), which is comparable to offshore concentrations of ~0.3 μM (Altabet, 1988).

Bulk net tow material (predominantly zooplankton) consistently had among the highest measured $\delta^{15}N$ of the analyzed N pools at each site, 2-3‰ higher than the $\delta^{15}N$ of PN. As with the other measured N pools, net tow $\delta^{15}N$ decreased from nearshore to the north rim by about 2.8‰ (Figure 3a; Table 1). Larger size fractions of zooplankton generally had a higher $\delta^{15}N$ than did smaller size fractions, with an average difference of roughly 1‰ between the largest and smallest fractions (Figure 3a).

3.1.3 Benthic autotrophs and heterotrophs

The three types of macroalgae examined were all similar in $\delta^{15}N$ at each site, decreasing from as high as 5‰ (*Laurencia* sp.) nearshore to as low as 1‰ (*Caulerpa* sp.) at the north rim (Figure 3d). For a generalized comparison, $\delta^{15}N$ was averaged across the three genera at each site. This average macroalgae $\delta^{15}N$ decreased from about 4.5‰ nearshore to 1.4‰ at the north rim (Table 1). Macroalgae and PN were similar in $\delta^{15}N$ at most sites, but

10.3389/fmars.2025.1554418

TABLE 1 $\delta^{15}N$ averages and gradient slopes of $\delta^{15}N$ *versus* the natural log of distance from known groundwater discharge.

	Average $\delta^{15}N$ (‰ *vs.* air)											$\delta^{15}N$ *vs.* ln (Distance)					
	Site A	SD	Site B	SD	Site C	SD	Site D	SD	Site E	SD	All	Slope	SE	Inter.	SE	R^2	n
P.ast. Bulk	5.00	0.34	4.65	0.32	3.04	0.28	2.61	0.06	2.43	0.13	3.55	-1.00	0.07	5.11	0.13	0.94	15
P.ast. Symb	5.76	0.45	4.74	0.30	3.64	0.09	3.50	0.23	2.77	0.26	4.08	-0.98	0.08	5.61	0.14	0.93	15
P.ast. Host	4.02	0.49	4.17	0.44	2.18	0.54	1.74	0.08	1.61	0.26	2.75	-1.02	0.12	4.33	0.22	0.85	15
P.ast. CS	7.02	0.28	6.34	1.00	4.42	0.22	4.13	0.14	4.17	0.13	5.21	-1.16	0.14	6.99	0.24	0.86	14
M.dec. Bulk	5.03	0.29	4.20	0.09	3.14	0.21	2.48	0.38	2.71	0.37	3.51	-0.89	0.08	4.90	0.15	0.90	15
M.dec. Symb	4.96	0.53	4.36	0.83	2.99	0.39	–	–	2.21	0.50	3.63	-1.01	0.14	4.98	0.24	0.83	12
M.dec. Host	4.66	0.37	3.75	0.13	2.74	0.37	2.27	0.23	2.38	0.27	3.16	-0.85	0.08	4.48	0.15	0.90	15
M.dec. CS	6.32	0.61	6.55	0.46	5.24	0.57	5.34	0.36	4.11	0.53	5.51	-0.75	0.15	6.67	0.28	0.66	15
D.lab. Bulk	6.20	0.05	5.22	0.16	3.69	0.39	3.35	0.03	3.29	0.22	4.35	-1.09	0.07	6.04	0.14	0.95	15
D.lab. Symb	5.45	0.44	4.31	0.15	2.79	0.22	2.87	0.22	2.42	0.06	3.57	-1.05	0.09	5.20	0.16	0.92	15
D.lab. Host	6.56	0.08	5.69	0.57	3.95	0.45	3.58	0.11	3.88	0.33	4.73	-1.08	0.12	6.40	0.22	0.87	15
D.lab. CS	6.01	0.20	4.92	0.49	4.72	0.18	3.98	0.28	3.46	0.39	4.62	-0.79	0.10	5.85	0.18	0.83	15
M.cav. Bulk	5.17	0.22	4.55	0.19	3.85	0.39	3.42	0.48	3.29	0.30	4.06	-0.67	0.07	5.10	0.14	0.86	15
M.cav. Symb	3.98	0.19	3.98	0.42	3.25	0.20	2.76	0.76	2.65	0.42	3.33	-0.55	0.11	4.19	0.22	0.65	15
M.cav. Host	5.11	0.24	4.33	0.50	3.76	0.39	3.36	0.39	3.45	0.20	4.00	-0.60	0.09	4.93	0.17	0.78	15
M.cav. CS	5.57	0.32	5.53	0.57	4.87	0.47	4.31	0.19	4.33	0.08	4.92	-0.51	0.09	5.71	0.17	0.72	15
Serpulids	6.17	0.19	5.70	0.22	4.74	0.33	3.76	0.38	3.75	0.15	4.82	-0.93	0.07	6.27	0.13	0.91	20
Net Tow	6.49	0.44	6.07	0.63	4.35	0.13	3.74	0.37	3.22	0.19	4.78	-1.22	0.08	6.67	0.15	0.92	21
PN	3.50	0.16	3.16	0.50	2.33	0.43	1.48	0.15	0.94	0.22	2.73	-0.90	0.08	3.68	0.15	0.88	19
Algae	4.46	0.58	3.51	0.40	2.02	0.29	1.60	0.33	1.42	0.51	2.66	-1.19	0.06	4.43	0.10	0.91	43

macroalgae $\delta^{15}N$ was roughly 1‰ higher than PN $\delta^{15}N$ at the site nearest to shore ($p < 1E-07$).

The serpulid worms exhibited a $\delta^{15}N$ trend similar to those of the other N pools described above, changing by about 2.5‰ across the platform. At each site, serpulid worm $\delta^{15}N$ was similar to zooplankton net tow $\delta^{15}N$ and 2-3‰ higher than PN $\delta^{15}N$ (Table 1). Perhaps as a result of the 1‰ elevation in macroalgae $\delta^{15}N$ relative to PN $\delta^{15}N$ at the innermost site, the difference between serpulid $\delta^{15}N$ and macroalgae $\delta^{15}N$ decreased from 2.3‰ at the outermost reefs to 1.4‰ at the reef nearest shore.

3.2 $\delta^{15}N$ gradient as a function of distance from the island

Distance was measured between each site and the ocean-adjacent edge of Bermuda's largest groundwater lens, the Devonshire (Vacher, 1978; Rowe, 1984), where groundwater discharge has been observed at the edge of the island in Tynes Bay (Sims et al., 2020). In linear regression models, the $\delta^{15}N$ of all N pools was significantly correlated with the natural log of distance from this groundwater lens ($p < 0.003$; Figure 5; Table 1).

In these regressions, almost all soft tissue N pools had similar slopes, ranging from about -0.8 to -1.2 (Table 1). Among the benthic organisms sampled, macroalgae showed the steepest gradient (Figure 5; Table 1). This was statistically different from its heterotrophic comparator, serpulid worms, though both are similar in scale ($p < 0.006$; Figure 5; Table 3).

For three of the coral species, the regression slopes for soft tissue components (i.e., bulk tissue, host animal tissue, and symbionts) were not statistically different from one another ($p > 0.09$). The exception was *M. cavernosa*, which had slightly lower slopes than the other three coral species ($p < 0.05$). Overall, the gradients in coral bulk tissue $\delta^{15}N$ more closely resembled that of serpulid worms than zooplankton net tows, with three species of coral not statistically different from the serpulid worms and just one species of coral not statistically different from the net tows (Table 3).

3.3 $\delta^{15}N$ of coral skeleton-bound organic matter compared to coral soft tissue

Geometric mean regression was used to plot coral tissue $\delta^{15}N$ against top-layer CS-$\delta^{15}N$ (Figure 6). Regression analyses are shown

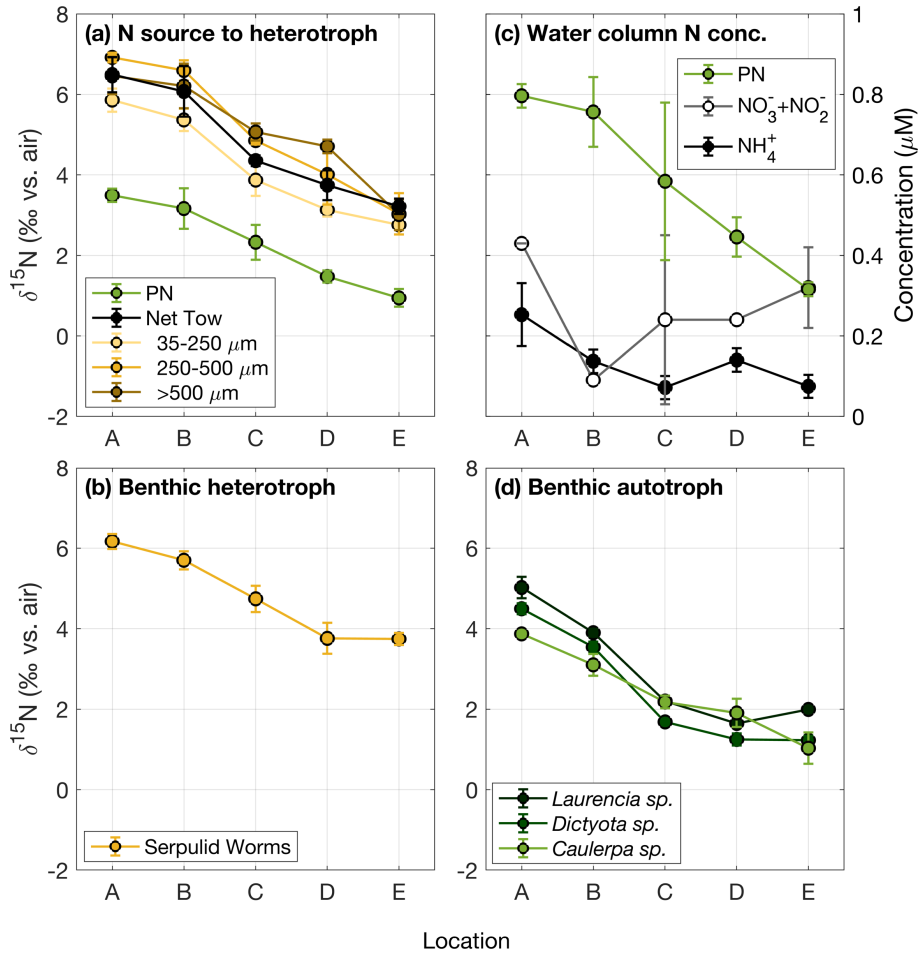

FIGURE 3
(a) $\delta^{15}N$ of heterotrophic sources of N in the water column, including PN and bulk and size-fractionated net tow material; **(b)** $\delta^{15}N$ of benthic heterotrophs; **(c)** DIN concentrations; and **(d)** $\delta^{15}N$ of three genera of benthic macroalgae. Locations correspond to those shown in Figure 1, with site A nearest to the island and site E farthest from the island at the northernmost rim.

both between CS-$\delta^{15}N$ and the $\delta^{15}N$ of coral bulk tissue (i.e., coral plus symbionts) and between CS-$\delta^{15}N$ and coral animal host tissue alone (Table 4). For all coral species, slopes were not statistically different from 1 using a 95% confidence interval.

Average offsets between coral host tissue $\delta^{15}N$ and CS-$\delta^{15}N$ varied among species, ranging from about 0‰ to 2.5‰, with a positive offset indicating that CS-$\delta^{15}N$ was higher than tissue $\delta^{15}N$. This offset was ~0-1‰ for the two coral species with large polyps and ~2.5‰ for the two coral species with small polyps sampled in this study (Table 4).

4 Discussion

4.1 Origin of the $\delta^{15}N$ gradient across the Bermuda platform

The data support the persistent presence of a $\delta^{15}N$ gradient across the Bermuda platform that is recorded in many different pools of organic matter. The $\delta^{15}N$ gradient is most likely anthropogenic, as argued previously by Baker et al. (2017). To date, Bermuda, an island of about 65,000 residents, does not have a national sewer system and has only limited sewage treatment facilities. Instead, there are two primary methods for wastewater management. The City of Hamilton, the island's urban center, has a wastewater management system, originally commissioned in 1920, that collects wastewater to a central point near the harbor and pumps minimally treated sewage into the open ocean on the south coast of the island (Corbett et al., 2002; Jones et al., 2011; Bermuda Ministry of Public Works, 2023). At the time of sampling, domestic properties not within the City of Hamilton were required to have their own deep, dug-in, unlined cesspits, which are specially designed to promote seepage into the limestone bedrock (Simmons et al., 1985; Jones et al., 2011). Bermuda has five fresh groundwater lenses, the largest of which is the centrally located Devonshire that covers more than twice the area of the other four lenses combined (Vacher, 1974, 1978; Plummer et al., 1976) and has an average nitrate concentration of 749 μM, attributable to sewage seepage (Vacher, 1974; Simmons, 1983; Simmons et al., 1985). The nitrate in this groundwater has relatively elevated $\delta^{15}N$ due to

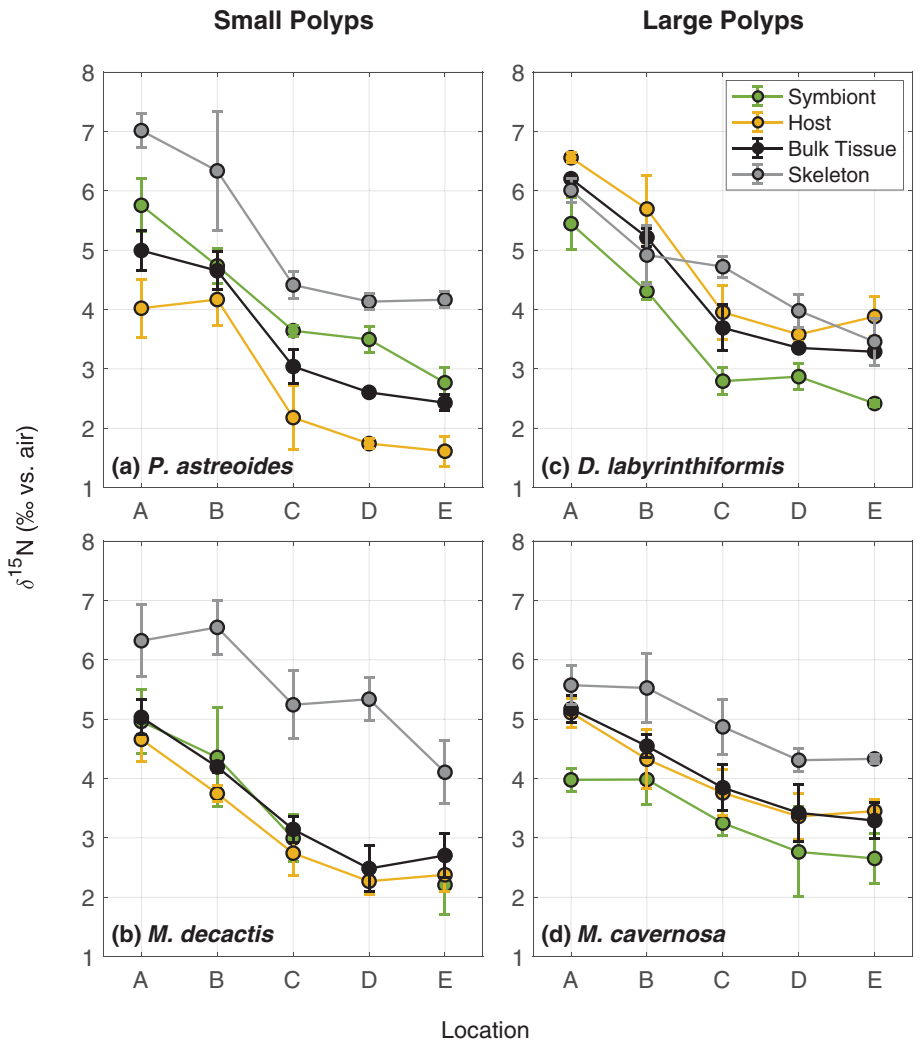

FIGURE 4
$\delta^{15}N$ of coral skeleton-bound organic matter, coral bulk tissue (i.e., host plus symbionts), coral host tissue, and coral endosymbionts for **(a)** *P. astreoides*, a mounding coral with small polyps, **(b)** *M. decactis*, a branching coral with small polyps, **(c)**, *D. labyrinthiformis*, a mounding brain coral with large polyps, and **(d)** *M. cavernosa*, a mounding coral with large polyps. Locations correspond to those shown in Figure 1, with site A nearest to the island and site E farthest from the island at the northernmost rim.

denitrification, which tends to elevate the $\delta^{15}N$ of the remaining nitrate substrate pool (Simmons and Lyons, 1994; Sims et al., 2020). At the bottom of a sample well in the Devonshire groundwater lens, Sims et al. (2020) measured groundwater nitrate plus nitrite concentrations of 635 µM with a $\delta^{15}N$ of 20‰. Across the Devonshire lens, ammonium concentration is negligible where nitrate concentration is high, and *vice versa* (Simmons et al., 1985), presumably depending on whether the groundwater conditions permit microbial oxidation of ammonium to nitrate ("nitrification").

TABLE 2 DIN concentrations across the reef sites on the Bermuda platform, also shown in Figure 3.

Site	Ammonium			Nitrate+Nitrite			PN		
	Conc. (µM)	SD	n	Conc. (µM)	SD	n	Conc. (µM)	SD	n
A (1 km)	0.25	0.08	4	0.43	0.10	2	0.80	0.03	4
B (2 km)	0.14	0.03	3	0.09	NA	1	0.76	0.09	3
C (6.5 km)	0.07	0.03	4	0.24	0.21	2	0.58	0.20	4
D (11 km)	0.14	0.03	3	0.24	NA	1	0.45	0.05	4
E (16.5 km)	0.07	0.03	4	0.32	0.00	2	0.32	0.02	4

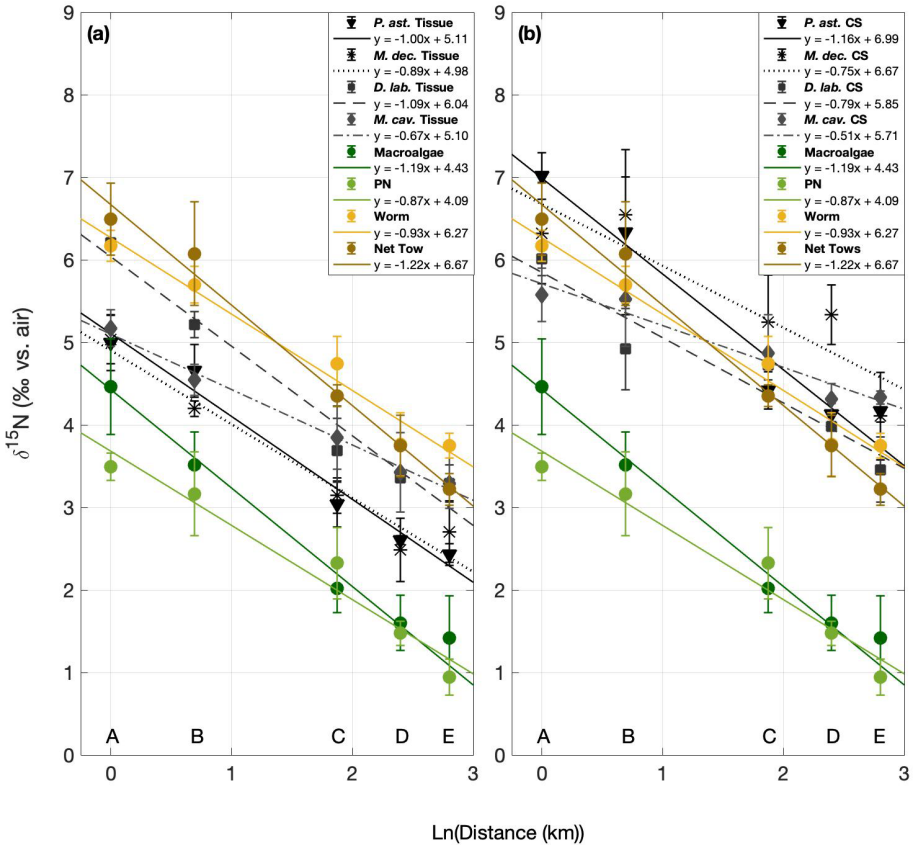

FIGURE 5
$\delta^{15}N$ summary shown *versus* the natural log of the distance from sites of known groundwater discharge, near the center of Bermuda's largest groundwater lens. Autotroph and heterotroph data are shown compared to the $\delta^{15}N$ of **(a)** coral host animal tissue and **(b)** coral skeleton-bound organic matter.

As the direct sewage outflow from the City of Hamilton is on the south shore of the island and the coral reefs studied across the Bermuda platform are to the north of the island, this is not likely to be an input of N to our study sites. Groundwater discharge, however, is likely to have a significant impact. Simmons and Lyons (1994) estimated an annual discharge of $1.1*10^{10}$ L of groundwater to Bermuda's inshore waters. Sims et al. (2020) observed groundwater discharge visually and by salinity measurement at one location and measured high nitrate concentrations up to hundreds of µM at the site of discharge, and up to 10 µM at 10 m away, with nitrate $\delta^{15}N$ as high as 11‰ at both sites. In addition, elevated $\delta^{15}N$ was measured in macroalgae and the tissue of corals from the nearshore waters of Tynes Bay. The high-nitrate groundwater discharge appeared to be mixed away quickly from the immediate vicinity, as nitrate concentration and $\delta^{15}N$ data across a transect perpendicular to the point of discharge suggested that the rapid drop in nitrate concentration moving away from shore was driven primarily by dilution rather than *in situ* consumption (Sims et al., 2020). However, the decrease in $\delta^{15}N$ with increasing distance from the island, in the context of reef waters with relatively low DIN concentrations (Figure 3c), suggests that most of the anthropogenic DIN is assimilated before being mixed off the pedestal. The high concentration of water column PN near the shore (0.8 µM) and the progressive decrease to near typical Sargasso Sea concentrations at the rim reef (0.3 µM; Figure 3c), without a comparable across-platform DIN gradient, are also consistent with complete consumption of coastally discharged N within the reef flat. Further, the strong correlation between the $\delta^{15}N$ and concentration of PN (Figure 7) is consistent with the transport of pollution-sourced N from inshore to offshore waters, largely as PN but with the potential for biological recycling of N between particulate and dissolved pools. Both natural and anthropogenic discharges of groundwater nitrate have been identified from N isotopic measurements in a range of modern reef environments (Duprey et al., 2017; Erler et al., 2018; Thibault et al., 2022; Choisnard et al., 2024; Erler et al., 2024). The case of the Bermuda platform is distinguished by the degree to which the isotopic signal appears to extend beyond the area of measurable groundwater nitrate.

4.2 Origin of the $\delta^{15}N$ relationships among N pools

Benthic macroalgae $\delta^{15}N$ was statistically different from PN $\delta^{15}N$ only at the site nearest the island, where macroalgae $\delta^{15}N$ was ~1‰ higher (Figure 5; Table 1). It is likely that the benthic macroalgae at that site provide a purer reflection of the input of high-$\delta^{15}N$ DIN from the island. By contrast, suspended PN is mixed

TABLE 3 Gradient slopes compared between components, with p-values indicating statistical difference between the two slopes.

	Serpulids	Net Tow	PN	Algae
P.ast. Bulk	0.424	0.055	0.355	0.040
P.ast. Symb	0.575	0.044	0.477	0.032
P.ast. Host	0.488	0.184	0.411	0.205
P.ast. CS	0.131	0.724	0.109	0.839
M.dec. Bulk	0.775	0.009	0.966	0.004
M.dec. Symb	0.603	0.211	0.511	0.233
M.dec. Host	0.644	0.003	0.664	0.001
M.dec. CS	0.306	0.009	0.383	0.008
D.lab. Bulk	0.121	0.234	0.092	0.288
D.lab. Symb	0.257	0.182	0.219	0.190
D.lab. Host	0.274	0.321	0.210	0.397
D.lab. CS	0.272	0.002	0.394	0.001
M.cav. Bulk	0.018	2E-05	0.045	1E-06
M.cav. Symb	0.008	4E-05	0.019	7E-06
M.cav. Host	0.006	1E-05	0.018	8E-07
M.cav. CS	8E-04	1E-06	3E-03	3E-08
Serpulids		0.009	0.780	0.006
Net Tow	0.009		0.008	0.764
PN	0.780	0.008		0.005
Algae	0.006	0.764	0.005	

Green indicates that the two slopes are not statistically different; red indicates statistically different slopes.

laterally with the water, which works to homogenize its $\delta^{15}N$, muting spatial $\delta^{15}N$ gradients that it might otherwise have due to N assimilation. In any case, the overall similarity in $\delta^{15}N$ between the macroalgae and the PN suggests that the latter is dominated by phytoplankton or phytoplankton-derived organic matter.

Serpulid $\delta^{15}N$ tracked the $\delta^{15}N$ pattern of PN but was 2-3‰ higher at each site across the platform (Figure 2; Table 1). The $\delta^{15}N$ of heterotrophic organisms is typically ~3‰ higher than that of the food source (DeNiro and Epstein, 1981; Minagawa and Wada, 1984). Thus, the elevation of serpulid $\delta^{15}N$ relative suspended PN $\delta^{15}N$ aligns with expectations, as serpulid worms primarily use filter feeding to consume small planktonic organisms such as dinoflagellates, algae, larvae and diatoms as well as detrital POM (Fauchald and Jumars, 1979; Jørgensen, 1996).

The $\delta^{15}N$ of zooplankton was roughly 2-3‰ higher than PN $\delta^{15}N$ across the platform, and thus similar to the $\delta^{15}N$ of serpulids. These relationships are consistent with zooplankton feeding predominantly on suspended POM. Indeed, zooplankton are thought to consume phytoplankton, detritus, and microzooplankton (e.g., Anraku and Omori, 1963; Richman et al., 1977; Lonsdale et al., 1979).

The bulk tissue $\delta^{15}N$ of corals with large polyps, *D. labyrinthiformis* and *M. cavernosa*, tended to be similar to or slightly lower than (1) the net tow material (i.e., zooplankton) and (2) the serpulid worms, at least at the three sites farthest from the island. This is consistent with the corals feeding mostly on zooplankton-sized organic matter and with endosymbiotic N recycling preventing a full trophic level $\delta^{15}N$ elevation relative to their N source (Wang et al., 2015). However, the range of possible food sources for corals leaves ambiguity as to the amplitude of the trophic $\delta^{15}N$ elevation associated with corals. For example, if the corals are feeding such that their N source has a $\delta^{15}N$ halfway between those of the net tow material and bulk suspended PN (i.e., is a 1-to1 mixture of the two), then we estimate a trophic $\delta^{15}N$ elevation for *D. labyrinthiformis* and *M. cavernosa* of <1‰ (Table 5). If, on the other hand, they feed dominantly on the bulk suspended PN pool, then we estimate a higher trophic $\delta^{15}N$ elevation for these two species of ~2‰ (Table 5). Assuming N uptake by feeding alone, then reliance on the net tow material alone would appear impossible in most cases, as the $\delta^{15}N$ of the corals tends to be lower than the net tow material, calling for an inverse trophic effect on $\delta^{15}N$ (Table 5), which has, to our knowledge, never been observed.

The $\delta^{15}N$ differences among different food sources may contribute to the $\delta^{15}N$ differences among coral species. In particular, the bulk tissue $\delta^{15}N$ of corals with small polyps, *P. astreoides* and *M. decactis*, was slightly lower than that of corals with large polyps (Figure 2). This might be explained by lower trophic $\delta^{15}N$ elevation for these two species, compared to the two coral species with larger polyps, with respect to the same sources of N (Table 5). However, if all coral species feed on a mixed diet of zooplankton and PN, lower coral $\delta^{15}N$ could also be achieved if the corals with smaller polyps feed on smaller zooplankton and/or feed more on suspended PN, which would result in a N source with overall lower $\delta^{15}N$ and no need for a different trophic $\delta^{15}N$ elevation. *P. astreoides*, in particular, is known for using mucus nets as an additional feeding mechanism (Lewis and Price, 1975; Brown and Bythell, 2005), which would largely capture the bulk PN pool as opposed to zooplankton. Moreover, corals with smaller polyps tend to capture fewer zooplankton than corals with larger polyps (Sebens et al., 1998; Palardy et al., 2006). An alternative explanation is that corals with small polyps, besides having different feeding strategies, are also more effective in recycling N internally, whereas large polyp corals may allow more ammonium leakage. Finally, in lab experiments, corals have demonstrated the capacity to assimilate forms of dissolved organic N (e.g., amino acids and urea; Grover et al., 2006, 2008). Given their low ambient concentrations in the environment, such dissolved organic N species are unlikely to be major contributors to the N nutrition of the coral host-symbiont system. However, they may be adequate to explain some of the inter-species $\delta^{15}N$ differences. Future work is needed to test these possibilities.

Corals clearly have the capacity to assimilate DIN (Muscatine and D'Elia, 1978; Webb and Wiebe, 1978; Wilkerson and Trench, 1986; Bythell, 1990; Marubini and Davies, 1996; Hoegh-Guldberg and Williamson, 1999; Grover et al., 2002, 2003; Badgley et al., 2006; Tanaka et al., 2006; Pernice et al., 2012; Kopp et al., 2013). It has been asserted that corals on tropical reefs rely more on DIN uptake

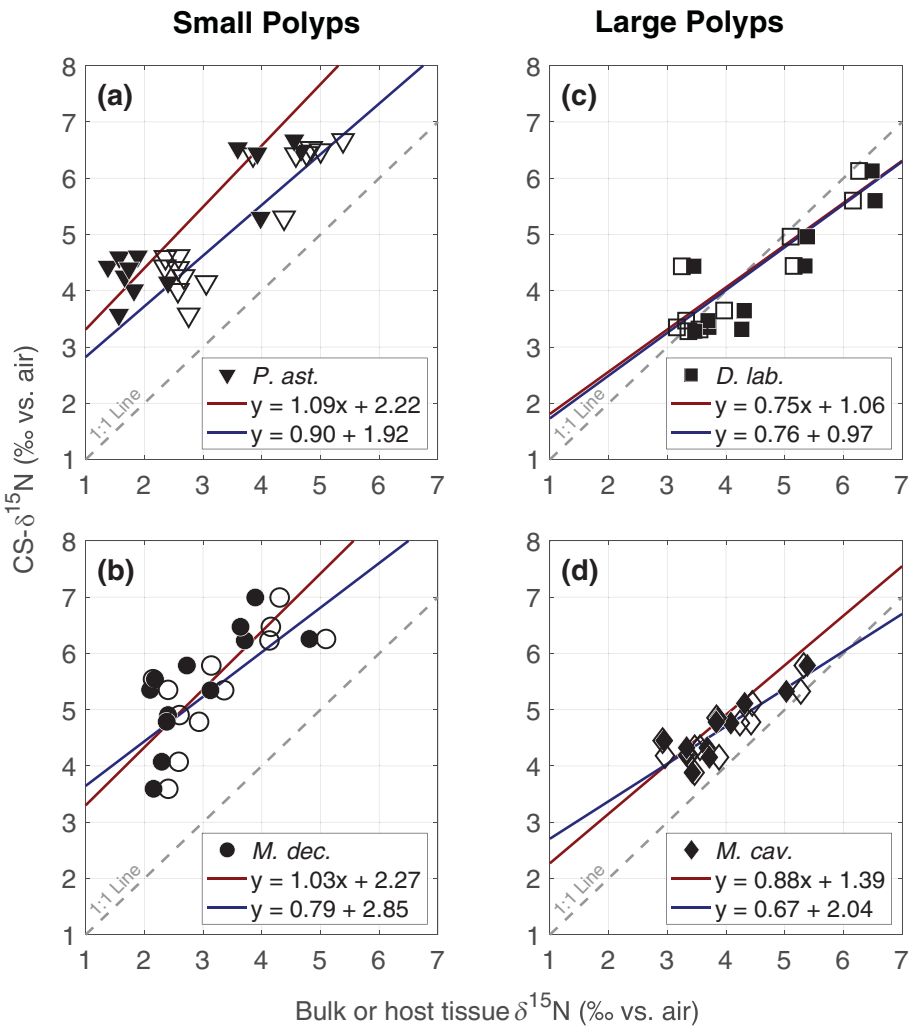

FIGURE 6
Coral skeleton-bound organic matter $\delta^{15}N$ *versus* coral tissue $\delta^{15}N$ for the four species studied. **(a)** *P. astreoides*, a mounding coral with small polyps, **(b)** *M. decactis*, a branching coral with small polyps, **(c)**, *D. labyrinthiformis*, a mounding brain coral with large polyps, and **(d)** *M. cavernosa*, a mounding coral with large polyps. Solid and open symbols reflect $\delta^{15}N$ measurements of host tissue and bulk tissue, respectively. Linear regression lines (red for host tissue, blue for bulk tissue) show a near 1:1 relationship between CS-$\delta^{15}N$ and tissue $\delta^{15}N$, with taxon-specific offsets.

TABLE 4 Average offsets (in ‰) between CS-$\delta^{15}N$ and coral bulk tissue and coral animal tissue, as well as linear geometric mean regressions.

	Average CS Offset	SE	Slope	SE	95% Confid. Interval	Intercept	SE	R^2
P.ast. Host	2.48	0.15	1.09	0.13	0.83 - 1.35	2.22	0.40	0.83
P.ast. Bulk	1.67	0.11	1.18	0.10	0.99 - 1.37	1.02	0.37	0.92
M.dec. Host	2.35	0.20	1.03	0.22	0.60 - 1.45	2.27	0.72	0.50
M.dec. Bulk	2.00	0.20	0.98	0.21	0.57 - 1.39	2.08	0.76	0.50
D.lab. Host	-0.12	0.21	0.75	0.14	0.48 - 1.03	1.06	0.68	0.60
D.lab. Bulk	0.27	0.16	0.78	0.12	0.55 - 1.00	1.24	0.52	0.73
M.cav. Host	0.92	0.09	0.88	0.12	0.64 - 1.13	1.39	0.50	0.76
M.cav. Bulk	0.87	0.11	0.83	0.13	0.58 - 1.08	1.56	0.52	0.72

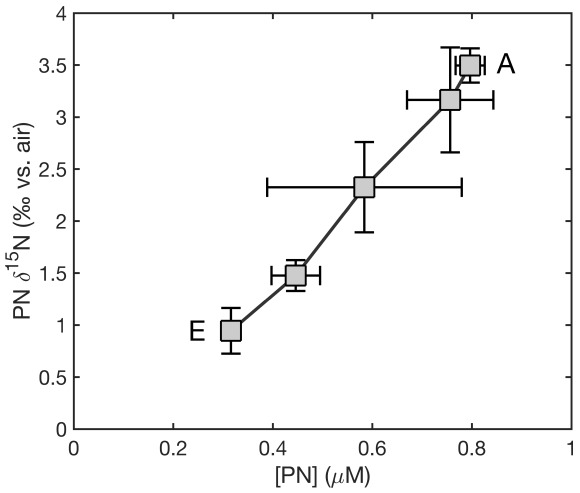

FIGURE 7
$\delta^{15}N$ *versus* concentration of water column-suspended PN across the Bermuda reef sites. Symbols are of the average values at each of the defined stations, with the line connecting each station to its closest neighbors, from nearshore (upper right) to the platform margin (lower left). Error bars reflect standard deviations for the measurements at each station.

TABLE 5 Estimated trophic elevation (in ‰) for coral species based on feeding from different pools.

Coral Species	Trophic Elevation based on N Source		
	Zooplankton	PN	50/50 Mix
P. astreoides	-1.23	1.26	0.02
M. decactis	-1.26	1.23	-0.02
D. labyrinthiformis	-0.43	2.07	0.82
M. cavernosa	-0.72	1.77	0.53

Values are calculated by subtracting the $\delta^{15}N$ of the food pool from coral bulk tissue $\delta^{15}N$ (i.e., coral system including symbionts) at each sample site and averaging across all sites. The $\delta^{15}N$ for a 50/50 food pool mix between zooplankton and PN is estimated as the average of zooplankton and PN $\delta^{15}N$.

by their photosymbionts than by feeding to maintain their symbioses (Wiedenmann et al., 2023). However, our data appear to rule this out for Bermuda corals. The coral $\delta^{15}N$ is 1-2‰ higher than macroalgae and PN. In contrast, if corals were assimilating the same DIN as macroalgae and phytoplankton and lack any other fractionating process, then they should have a $\delta^{15}N$ similar to those autotrophic N pools. There are only two scenarios in which this would not be the case: (1) DIN assimilation occurs with lower isotopic fractionation when conducted by corals than by macroalgae and phytoplankton, or (2) Corals excrete low-$\delta^{15}N$ N back into the environment. Existing data on isotopic fractionation argues against the first possibility. If anything, the existing studies suggest stronger isotopic fractionation for DIN assimilation by corals than by macroalgae (Swart et al., 2014; Devlin, 2015), which would tend to render coral tissue $\delta^{15}N$ lower than macroalgal $\delta^{15}N$. While phytoplankton consume both nitrate and ammonium with substantial isotopic fractionation when these substrates are at high concentration (e.g., Waser et al., 1998), these fractionations appear to decrease sharply at lower substrate concentrations (Pennock et al., 1996; Granger and Mathuri, 2021). The second possibility – DIN excretion by corals – is unlikely for mechanistic reasons. Specifically, if corals are actively assimilating DIN at the sub-micromolar concentrations of the reef waters, it would be highly maladaptive for them to also excrete DIN into the environment. It is possible that a small fraction of the Bermuda coral's N nutrition comes from DIN, but the data rule out dominant reliance on it. Rather, our data are most consistent with a feeding-dominated strategy for N acquisition by the coral host/symbiont system, with the $\delta^{15}N$ relationships suggesting that corals rely on some combination of suspended PN and net tow material.

Most previous studies documenting the capacity of corals to assimilate DIN were conducted under conditions with no feeding and/or DIN concentrations that are orders of magnitude higher than those observed in oligotrophic reefs, both conditions that would likely upregulate DIN assimilation. In an incubation experiment in 0.2 μM $^{15}NH_4^+$, Grover et al. (2002) showed that, when corals were fed, ammonium uptake became negligible and much lower than in the starved colonies. Even without feeding, Grover et al. (2003) found that nitrate uptake rates were six times lower in 0.3 μM $^{15}NO_3^-$ incubations (reef levels) compared to 3 μM $^{15}NO_3^-$ incubations, at less than 0.1 nmol hr^{-1} cm^{-2}. Based on the N biomass of the corals quantified by the authors, this equates to uptake of about 0.1% day^{-1}. Tanaka et al. (2018) estimated an overall N turnover rate of 0.27% day^{-1} for symbiotic corals in environmental conditions, which suggests that corals rely on more than just DIN uptake to meet their N needs in the natural environment. Two other short-timescale experiments at low DIN concentrations have estimated slightly higher nitrate uptake rates, ranging from 1 to 5 nmol cm^{-2} h^{-1} at ambient concentrations of 0.1-0.3 μM, which are typical of (or arguably at the high end) of oligotrophic reefs such as Bermuda (Bythell, 1990; Badgley et al., 2006). In one of these experiments, based on estimated N biomass of the coral species (Mills, 2000), this equates to the coral taking up an amount of nitrate equivalent to up to 0.33% of its biomass each day (Badgley et al., 2006), which is more comparable to the N turnover rate estimated by Tanaka et al. (2018). However, these experiments did not filter the seawater used for incubations. In this case, the estimated DIN uptake rates discussed likely include a contribution from phytoplankton that have assimilated ^{15}N tracer, leading to overestimation of the coral DIN uptake rate. Finally, Wiedenmann et al. (2023) performed 8-month-long $^{15}NO_3^-$ incubations of three coral species at nitrate concentrations of ~12 μM, observing substantial nitrate assimilation. However, the incubation water was filtered to reduce the particle load, which, as with prior incubation studies (e.g., Grover et al., 2002, 2003), meant that the experiments cannot speak to coral nitrate assimilation rates under typical reef conditions in which zooplankton and other particles are available for feeding. In the future, to advance our understanding of N acquisition in ocean surface waters, tracer isotope incubation experiments should control and vary the concentrations of both DIN and particulate food sources. The existing body of incubation studies do not make a

compelling case that coral DIN uptake is significant in the nutrient-poor surface waters of the tropical and subtropical reefs, such as those of Bermuda. Of course, substantial DIN assimilation may well occur in nutrient-rich reefs.

4.3 Origin of the $\delta^{15}N$ gradients in the N pools and corals

A major initial motivation for this study was the existing evidence for a $\delta^{15}N$ gradient across the Bermuda platform (Wang et al., 2015; Baker et al., 2017). Both Wang et al. (2015) and Erler et al. (2015) reported differences between CS-$\delta^{15}N$ gradients across reef transects in Bermuda and Heron Island, respectively, and the $\delta^{15}N$ gradients of other N pools measured across those respective sites, including zooplankton, macroalgae, PN, and nitrate. These studies hypothesized that the observed differences were due to changes in coral trophic $\delta^{15}N$ elevation across the transects as a result of differences in food availability. However, in the present study, we find only very modest differences between the $\delta^{15}N$ gradients of various coral N pools and the $\delta^{15}N$ gradients of benthic autotrophs (macroalgae) and heterotrophs (serpulid worms) that are also integrating N patterns over time. This observation from our study bodes well for the use of coral-bound N as a tool to reconstruct past changes in environmental $\delta^{15}N$, and it suggests that the trophic $\delta^{15}N$ elevation may be more stable than previously suspected.

At the same time, there may be information in the modest differences in the gradients that are observed among the N pools and corals. Comparison of these $\delta^{15}N$ gradients, which we statistically estimate using linear regression slopes, with those observed in the corals may provide additional insight into coral N sources. We begin by considering non-corals.

The $\delta^{15}N$ gradient in serpulid worms is indistinguishable from that in suspended PN, both of which are weaker than that of macroalgae (Figure 5; Table 1). It is not surprising that the macroalgae $\delta^{15}N$ gradient is stronger than that of serpulid worm $\delta^{15}N$, owing to the different sources of N for the two pools. We did not directly measure the DIN $\delta^{15}N$, both because of measurement limitations at low concentrations and because, at such low concentrations, the DIN $\delta^{15}N$ is likely to vary greatly due to short-term variation in consumption and resupply (e.g., Fawcett et al., 2015). Instead, we use the benthic macroalgae as a temporally integrative measure of the $\delta^{15}N$ of DIN supply at a given location on the platform (Yamazaki et al., 2011b). As discussed in section 4.2, the DIN $\delta^{15}N$ gradient is likely driven by nitrate input at the island (Sims et al., 2020) and is discussed further in Section 4.4. Benthic macroalgae, which are fixed in location, assimilate N from the DIN pool and should largely reflect that gradient. On the other hand, the PN $\delta^{15}N$ gradient is weaker ($p = 0.005$; Table 3). This weaker gradient can be explained by mixing, as the PN is mixed and circulated across the platform, which works to homogenize the pool. Serpulid worms, which are fixed in location, acquire N by filter feeding on PN and so reflect this slightly weakened $\delta^{15}N$ gradient ($p = 0.780$; Table 3).

In contrast, the gradient in net tow material is stronger than in suspended PN and thus more similar to that of macroalgae (Figure 5; Table 1). We propose that this is due to the ability of many organisms in the net tow material to migrate toward food sources and/or to hold their position against the homogenizing effects of mixing (Yamazaki and Squires, 1996; Schmitt and Seuront, 2001; Seuront et al., 2004; Genin et al., 2005; Visser, 2007). For example, this allows zooplankton in the nearshore waters to remain in this location and thus benefit from (and record) the high $\delta^{15}N$ food in this region. Notably, the strongest gradient that they can record is that of their food. Thus, this explanation requires one of the following two options. First, zooplankton may be feeding on benthic algal material. Second, zooplankton may be selecting prey items from the bulk suspended PN that were more recently produced and thus capture the $\delta^{15}N$ gradient of DIN across the platform more fully than does the $\delta^{15}N$ of the bulk PN. Some laboratory experiments have suggested that, in addition to selection based on particle size, some species of copepods are capable of selecting live algae over dead algae (DeMott, 1988, 1995). Bouillon et al. (2000) tested this idea in the natural environment, suggesting on the basis of seasonal and spatial variations in carbon isotope data that the zooplankton in mangrove ecosystems preferentially consume locally produced phytoplankton despite large amounts of terrestrial and mangrove detritus present in the water.

Like benthic macroalgae and serpulid worms, corals are fixed in location. For three of the coral species, the $\delta^{15}N$ gradients for all coral components (i.e., bulk tissue, host animal tissue, symbionts, and skeleton-bound N) were not statistically different from serpulid worms ($p > 0.12$; Table 3). The exception was *M. cavernosa*, which had slightly weaker gradients than the other three coral species ($p < 0.02$) and is discussed below. The macroalgae $\delta^{15}N$ gradient was typically stronger than the coral $\delta^{15}N$ gradients as well as the serpulid worm $\delta^{15}N$ gradient (Tables 1, 3). Among the coral components of greatest relevance, bulk tissue and skeleton-bound N, only *D. labyrinthiformis* bulk tissue $\delta^{15}N$ and *P. astreoides* CS-$\delta^{15}N$ gradients were not statistically different from the macroalgae $\delta^{15}N$ gradient. There are two possible explanations for these observations. First, corals are acquiring their N mostly from feeding. Second, corals are acquiring a significant portion of their N through DIN uptake by their symbionts, but the DIN $\delta^{15}N$ gradient is sometimes weaker than in our sampling period, and the long N turnover time of corals results in a weaker $\delta^{15}N$ gradient compared to macroalgae. We favor the first explanation, as the second arbitrarily invokes specific temporal changes in the DIN $\delta^{15}N$ gradient that have not been demonstrated. Thus, this comparison of the $\delta^{15}N$ gradients in the different N pools provides additional support for corals' reliance on feeding, rather than DIN assimilation, for their N.

In summary, the data suggest that coral tissue $\delta^{15}N$ and CS-$\delta^{15}N$ capture broad changes in environmental fixed N $\delta^{15}N$ about as well as other benthic heterotrophs do, and that the relationship between a given coral species and its endosymbionts does not change significantly for some range of differing environmental conditions, such as those observed across the Bermuda platform. As the coral $\delta^{15}N$ gradients are quite similar to the $\delta^{15}N$ gradients of benthic autotrophs and heterotrophs as well as potential heterotrophic food sources, there is no evidence in the present

study to support the cross-platform change in the $\delta^{15}N$ relationship of corals relative to N sources proposed by Wang et al. (2015) and Erler et al. (2015). Across the Bermuda platform, Wang et al. (2015) observed a much weaker net tow $\delta^{15}N$ gradient but a coral $\delta^{15}N$ gradient similar to that of the present study, suggesting the $\delta^{15}N$ gradients in water column pools may be variable and providing a possible explanation for the difference in conclusions. In any case, the data reported here increase confidence in the ability of CS-$\delta^{15}N$ to provide long-term records of changes in environmental N.

4.4 Differences in cross-platform $\delta^{15}N$ gradient among coral species

Among the four species, *M. cavernosa* was the only one for which the $\delta^{15}N$ gradient across the platform was statistically different, being marginally weaker than the others. This was driven primarily by the two sites closest to the island, where *M. cavernosa* $\delta^{15}N$ was not as elevated as the other species with large polyps, *D. labyrinthiformis*, becoming more similar in $\delta^{15}N$ to the corals with small polyps. This might be explained by the increased turbidity and higher concentration of suspended particles at the nearshore sites, interacting with differences in particle selection between *D. labyrinthiformis* and *M. cavernosa*. Both *D. labyrinthiformis* and *M. cavernosa* have been described as effective at using their tentacles to capture zooplankton prey and mucus strands to capture suspended particles. However, *M. cavernosa* is also notably adept at consuming settling particles that fall into its open mouths due to the funnel shape of the polyp cup (Lewis and Price, 1975). Studies comparing particle ingestion found that a similar species, *Montastrea franksi* (later taxonomically revised to *Orbicella franksi*), has much higher rates of ingestion of both suspended and deposited particles compared to three other coral species, including another species of *Diploria* (later taxonomically revised to *Pseudodiploria;* Mills et al., 2004). Thus, it is possible that the diet of *M. cavernosa* shifted toward generic organic particles in the turbid waters near the island, resulting in a slightly lower bulk tissue $\delta^{15}N$ than its counterpart, *D. labyrinthiformis*.

While we have argued above that DIN assimilation cannot be the principal mechanism by which corals acquire N across the Bermuda platform, it is possible that inter-species differences in $\delta^{15}N$ and in cross-platform $\delta^{15}N$ gradients are affected by a small amount of DIN assimilation. In the case of the Bermuda platform, changes in isotopic fractionation are unlikely because of the relatively constant (low) DIN concentrations and sample depths across the platform (Figure 3c). However, differences among species in the proportion of the corals' N that is derived from DIN may still affect coral $\delta^{15}N$ patterns across the platform. As suggested by the difference between macroalgae and serpulid worm $\delta^{15}N$ across the platform, reliance on DIN results in a stronger $\delta^{15}N$ gradient than utilization of water column PN. Following this logic, the differences in $\delta^{15}N$ gradient among the coral species may also relate to PN *versus* DIN use, with greater use of DIN resulting in a stronger $\delta^{15}N$ gradient. However, while this may help to explain the differences in $\delta^{15}N$ gradient among the coral species, this mechanism would not explain the $\delta^{15}N$ differences among N pools at each site, thus making a changing food source for *M. cavernosa* the more likely explanation.

4.5 Relationship between coral host tissue and endosymbiont $\delta^{15}N$

For each of the four species, the $\delta^{15}N$ difference between endosymbionts and the host tissue (Δsymb-host) is well conserved across the platform, with relatively few exceptions. However, there are substantial inter-species differences in Δsymb-host, ranging from ≤-1‰ in *D. labyrinthiformis* to >+1‰ in *P. asteroides*. Δsymb-host has been investigated abundantly in previous work (e.g., Erler et al., 2015; Conti-Jerpe et al., 2020; Fujii et al., 2020; Thibault et al., 2022), although there is not yet consensus on its controls. Simplistically, the observation that Δsymb-host is typically negative could be interpreted to reflect the low $\delta^{15}N$ of the metabolic N provided from the host to the endosymbionts. However, Δsymb-host varies, with positive and negative values occurring across taxa. This is perhaps to be expected, as Δsymb-host should be sensitive to a range of processes and their isotopic characteristics, including both the transfer of metabolic N from the host to the symbiont and the transfer of photosynthetically produced organic N back to the host.

Our findings of a relatively well-conserved Δsymb-host for each coral species across the platform (Figure 7) argue for a relatively short list of primary controls. The platform sites cover a substantial range of environmental conditions, for example, in the concentration of PN (Figure 3c; and thus likely also particulate carbon concentration). Thus, if many processes contribute strongly to Δsymb-host, we might have expected more inter-site variability in Δsymb-host. Our preferred interpretation is that Δsymb-host is dominantly controlled by the $\delta^{15}N$ of the organic N that is translocated from symbionts to host, such as might relate to the large $\delta^{15}N$ differences observed among the amino acids. For example, the species differences in Δsymb-host could be explained by differences in the dominant amino acids translocated from the symbionts. As described below, such variation in the $\delta^{15}N$ of translocated N from symbiont to host might also help to explain an apparent relationship between Δsymb-host and skeleton-bound N $\delta^{15}N$. However, we caution that other interpretations for the controls on Δsymb-host have been proposed (e.g., Conti-Jerpe et al., 2020). For example, there is evidence that, in some coral taxa, amino acids from ingested food can be passed directly to the symbionts Martinez et al., 2022).

Despite the many uncertainties, the occurrence of positive Δsymb-host is a potentially useful constraint on coral nutrition. The metabolic ammonium available to the symbionts is likely to be lower in $\delta^{15}N$ than the host tissue (Wang et al., 2015), explaining the tendency in most cases for Δsymb-host to be negative (e.g., Conti-Jerpe et al., 2020). If so, a positive Δsymb-host implies that the $\delta^{15}N$ of the N being returned to the host is higher in $\delta^{15}N$ than the symbiont. This argues against assertions that the coral host receives organic N from the symbionts largely by direct feeding on

the symbionts (Wiedenmann et al., 2023). Rather, it favors the return of specific compounds from the symbiont to the host.

4.6 Relationship between coral soft tissue and skeleton-bound $\delta^{15}N$

Geometric mean regressions between coral tissue $\delta^{15}N$ and top-layer CS-$\delta^{15}N$ of each coral species suggest a roughly one-to-one relationship between the two, with some offset. This result is not surprising, as the one-to-one relationship is the default expectation given the existing understanding of the calcification process. It has long been recognized that the calcium carbonate skeleton of hard corals contains organic material trapped during the mineralization process (Goreau, 1959). Although the relative importance of the organic and inorganic aspects of calcification have been debated, it is generally believed that corals' calcification process is biologically mediated (reviewed in Tambutté et al., 2011; Falini et al., 2015). To not have a one-to-one relationship, the organic matter involved in the skeletal accretion process would have to be changing in its relationship to coral tissue as a result of environmental conditions, which would be unlikely for a biochemically regulated process. Research is ongoing as to the role, composition, and origin of the organic molecules, or "organic matrix," within corals' calcium carbonate skeleton (e.g., DeCarlo et al., 2018). In any case, our data add to the growing evidence that there is a high degree of correlation between coral host tissue $\delta^{15}N$ and CS-$\delta^{15}N$ (Erler et al., 2015).

There does appear to be an offset between coral host tissue $\delta^{15}N$ and CS-$\delta^{15}N$, the magnitude of which varies among coral species. This offset is ~0-1‰ for the corals with large polyps and just under 2.5‰ for the corals with small polyps sampled in this study (Table 4). Previous studies also observed different offsets between coral tissue $\delta^{15}N$ and CS-$\delta^{15}N$ among different species of corals (Erler et al., 2015; Hoegh-Gulberg, 2004). Hoegh-Gulberg (2004) observed a wide range of offsets for the two coral species studied under various long-term nutrient enrichment conditions up to 100 times higher than natural concentrations, with coral tissue ranging from being 2‰ lower to 2.5‰ higher than CS-$\delta^{15}N$ depending on the nutrient condition. However, entire coral heads >15 cm in diameter were used in that study, and it is unknown how variable the CS-$\delta^{15}N$ may have been over the course of the coral's life. Moreover, their dialysis-based method of CS-N isolation may have lost portions of the CS-N pool, such that the results may not be fully comparable with the present study. Erler et al. (2015) sampled coral skeleton more selectively, from just below the tissue, and observed offsets of about 0‰ to 1.1‰ for two different species of coral, *Favia stelligera* and *Porites lutea*. For both Erler et al. (2015) and the present study, corals with small polyps tended to have a larger tissue-CS-$\delta^{15}N$ offset than corals with large polyps.

It is not immediately clear why there is taxonomic variation in the tissue-CS-$\delta^{15}N$ offset. One plausible explanation for the variation in tissue-CS-$\delta^{15}N$ offset is that there are slight taxonomic differences in the complex process of biomineralization. The amino acid ratios of the coral skeletal organic matrix protein assemblage have been shown to be different among different coral species (Young et al., 1971; Ingalls et al., 2003; Puverel et al., 2005). Large $\delta^{15}N$ differences are observed among amino acids, presumably largely due to involvement in deamination and transamination reactions (reviewed by O'Connell, 2017). While the dynamics are still being understood in heterotrophic organisms, the "trophic" amino acids (typically, glutamic acid, alanine, aspartic acid, proline, leucine and valine) have higher $\delta^{15}N$ than do "source" amino acids (typically, phenylalanine, glycine, serine, tyrosine, lysine, methionine and histidine) (Popp et al., 2007; Nielsen et al., 2015). Differences in proportions of amino acids in the organic matrix within the coral skeleton could explain $\delta^{15}N$ offsets between coral tissue $\delta^{15}N$ and CS-$\delta^{15}N$. For example, in *Porites lutea*, Ingalls et al. (2003) observed proportionally more than four times as much aspartic acid (typically higher in $\delta^{15}N$) in the intracrystalline organic matter compared to polyp tissue, and less than half as much phenylalanine, serine, tyrosine, and histidine (typically lower in $\delta^{15}N$). This is a possible explanation for the higher $\delta^{15}N$ observed in CS-$\delta^{15}N$ relative to coral host tissue for species of *Porites*. In addition to the observed differences in coral skeletal organic matrix amino acid assemblages, proteomic work has suggested that there are coral-specific proteins involved in the calcification process and that specific pathways of skeletal synthesis exist among biomineralizers (Drake et al., 2013; Mass et al., 2016). A recent study has added evidence to the existence of a "core set" of proteins fundamental to scleractinian biomineralization (Zaquin et al., 2021). It also identified lineage-specific and species-specific proteins and organic matrix frameworks that may play a significant role in morphology differences between coral species, supporting the biochemical feasibility of taxon-specific coral skeletal synthesis processes.

It has been suggested that the symbionts may play a special role in promoting production of and/or may contribute directly to the organic matrix (reviewed in Davy et al., 2012), though evidence for this is not clear (Inoue et al., 2018). Aspects of our data appear consistent with the possibility of a direct contribution (e.g., of specific amino acids). In particular, across taxa, we observe a positive correlation between the $\delta^{15}N$ difference between skeleton-bound N and host tissue (ΔCS-host) and Δsymb-host (Figure 8). This suggests that there is some degree of dependence of the CS-$\delta^{15}N$ on the symbiont $\delta^{15}N$, in addition to the strong dependence that CS-$\delta^{15}N$ has on host tissue $\delta^{15}N$.

At the same time, there have been suggestions that fossil-bound organic matter could include environmental organic matter. ^{14}C labelling experiments indicate that corals can take up aspartic acid from the water column and incorporate it into the skeletal organic matrix (Allemand et al., 1998). Comparisons to abiogenic carbonates have been used to suggest that other types of seawater-sourced organic matter may be incorporated as well (DeCarlo et al., 2018). Such a range of possibilities underscores the need for further investigation of the mechanisms of coral calcification and their implications for coral skeleton-bound organic matter.

Another consideration is that coral tissue "turns over" on a time scale of ≥3 months (Rangel et al., 2019) while the coral skeletal organic matrix is added permanently at the time of calcification. Given our coral skeleton sampling approach, the measured CS-$\delta^{15}N$ sampling likely reflects at least a few years of coral calcification.

Accordingly, if there are seasonal or even interannual changes in the N cycle on the Bermuda platform, then our tissue and skeleton-bound organic matter measurements may include offsets due to the differences in the time periods that they represent. This is yet another possibility for the offsets that requires future work to address.

In sum, the nearly one-to-one linear relationship between coral host tissue $\delta^{15}N$ and CS-$\delta^{15}N$ and overall fidelity to the $\delta^{15}N$ patterns of the environment suggest that CS-$\delta^{15}N$ is able to record relative changes in environmental $\delta^{15}N$. However, the species-specific tissue-CS $\delta^{15}N$ offsets suggest that species should be considered carefully in the generation of CS-$\delta^{15}N$ records.

We also note that the coefficient of determination (R^2) of the linear regressions between coral host tissue $\delta^{15}N$ and CS-$\delta^{15}N$ ranged from 0.50 to 0.92. Some of the lower R^2 values, indicating greater variance, may be due to the approximate nature of the sampling method used. *M. decactis*, the branching coral, had the lowest R^2 of the coral species examined. It was also the most difficult to sample in a consistent manner because of the curved trajectories of the corallites in the accretive growth process of the branches (Kaandorp et al., 2005), and it was likely the most inconsistently sampled in terms of the amount of time captured in a single skeletal sample. For the other three mounding species, we consistently sampled to the same depth in the skeleton along the growth axis, but this may not have captured the same amount of time owing to slight differences in coral growth rates across the platform. Previous work has shown that *P. astreoides* and *D. labyrinthiformis* have higher growth rates nearer to shore (near Site D of this study) than at the rim reef (near Site E of this study), and this difference is more pronounced in *D. labyrinthiformis* (Courtney et al., 2017). This discrepancy may help to explain the relatively lower R^2 of *D. labyrinthiformis* compared to *P. astreoides*.

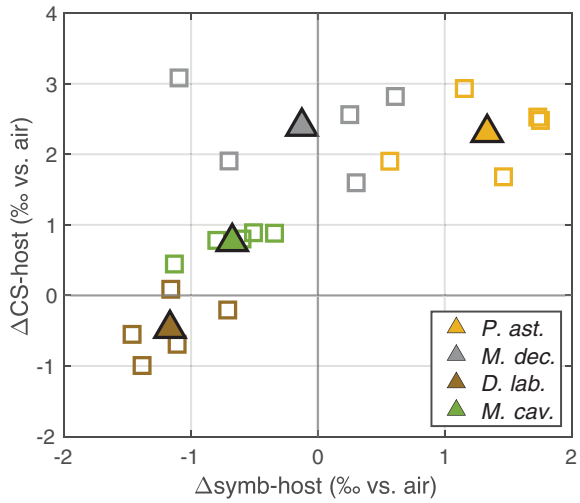

FIGURE 8
The $\delta^{15}N$ difference between coral skeleton-bound N and the host tissue (ΔCS-host) *versus* the difference between the symbionts and the host tissue (Δsymb-host). For each coral species studied (see legend), open squares reflect individual stations, and filled triangles are the cross-platform average.

For all of the above complexities and considerations, it is remarkable that the relationship of CS-$\delta^{15}N$ to water column PN $\delta^{15}N$ is similar across the multiple species (Figure 5b). As yet, we do not know of a mechanism by which coral tissue-to-PN $\delta^{15}N$ differences would be compensated by CS-to-coral tissue $\delta^{15}N$ differences to yield this simple observation, and it may be a coincidence. Future work should pursue this result, which, on its face, would appear optimal for the fidelity of environmental reconstructions.

5 Conclusion and perspective

Our N isotopic measurements of corals and other organisms and N pools across the Bermuda platform confirm a previously identified $\delta^{15}N$ increase toward the Bermuda coast and make use of that gradient to gain insights into the N sources of corals and the signals recorded by CS-$\delta^{15}N$. The $\delta^{15}N$ of bulk coral tissue is consistent with corals feeding dominantly on some combination of zooplankton-sized organic matter and smaller PN. Depending on the relative importance of these two sources, the trophic $\delta^{15}N$ elevation of the corals is between 0 and 0.5-1.5‰. This range of values is well below the typical trophic $\delta^{15}N$ elevation of a heterotroph (of ~3-4‰; Post, 2002), consistent with the recycling and retention of low-$\delta^{15}N$ metabolic N by symbiont-bearing corals. Comparison of the coral data with $\delta^{15}N$ data from benthic macroalgae argues against corals' significant reliance on the DIN. We consider these data as strong support for the dominance of coral feeding over DIN assimilation in this and other nutrient-poor reef settings, despite recent arguments to the contrary (Wiedenmann et al., 2023).

In our view, these results conform with the adaptive benefits of the coral-zooxanthellae symbiosis. The coral host is a benthic animal typically occurring in sunlit and nutrient-depleted low latitude surface waters in which phytoplankton growth is limited by the "major" nutrients, nitrogen and phosphorus. Its feeding and metabolism naturally concentrate these nutrients within their tissues, as is true for all heterotrophic organisms, in which the net reaction is respiration. Mutual benefit can be found in harboring algal symbionts that use this concentrated stream of metabolically produced nutrients to fuel photosynthetic growth, with a portion of the resulting organic matter returning to the coral host. Thus, from the perspective of the coral host, their feeding provides chemical energy more than once, as the metabolic production of inorganic nutrients fuels symbiont growth. In contrast, dissolved inorganic nutrient uptake in nutrient-poor tropical and subtropical waters is challenging for phytoplankton, and it should be even more challenging for corals, in which the symbiont requiring these nutrients is isolated by multiple membranes, their own and their hosts, from the external nutrients. There are nutrient-rich surface waters over some coral reefs (e.g., those in the eastern equatorial Pacific as well as in human-impacted coastal regions), where DIN acquisition would be easier, and corals might assimilate DIN under these conditions. However, these environments are also often highly productive and characterized by relatively higher POM and zooplankton concentrations. Consequently, corals inhabiting these environments would have access to abundant organic nitrogen through feeding. In any case, we find the morphological and

behavioral differences between symbiotic corals and free-living phytoplankton to point to feeding-driven nutrient supply coupled with internal nutrient recycling as an important coral growth strategy.

Among the four coral species investigated, two species with smaller polyps (1-2 mm) have ~1‰ lower bulk tissue $\delta^{15}N$ than two counterparts with larger polyps (5-10 mm). Differences in the proportions of food sources are a possible explanation. However, there are many other possibilities, including small inter-species differences in DIN assimilation. Taxon-specific $\delta^{15}N$ differences are also observed between coral tissue and skeleton-bound N, with larger differences in the two small-polyp species. Surprisingly, accumulating these differences yields CS-$\delta^{15}N$ mean values and spatial gradients that were similar in the four species studied. This bodes well for CS-$\delta^{15}N$ as a proxy for N isotopic changes in the marine environment. However, the result may be fortuitous, and a mechanistic explanation is required to explain the compensation among differences that led to it. These field-based ground-truthing data on CS-$\delta^{15}N$ may become better understood with more information from experiments on the biochemical pathways associated with the incorporation of coral-bound organic matter as well as its chemical composition.

Data availability statement

The original contributions presented in the study are included in the article. Further inquiries can be directed to the corresponding author.

Ethics statement

The manuscript presents research on animals that do not require ethical approval for their study.

Author contributions

VL: Conceptualization, Formal analysis, Investigation, Methodology, Project administration, Visualization, Writing – original draft, Writing – review & editing. YR: Methodology, Visualization, Writing – original draft, Writing – review & editing. WD: Investigation, Writing – original draft, Writing – review & editing. SO: Methodology, Writing – original draft, Writing – review & editing. SP: Investigation, Methodology, Resources, Writing – original draft, Writing – review & editing. AC: Conceptualization, Funding acquisition, Investigation, Methodology, Project administration, Resources, Supervision, Writing – original draft, Writing – review & editing. XW: Conceptualization, Writing – original draft, Writing – review & editing. DS: Conceptualization, Funding acquisition, Methodology, Resources, Supervision, Writing – original draft, Writing – review & editing.

Funding

The author(s) declare that financial support was received for the research and/or publication of this article. This work was supported by the US NSF Graduate Research Fellowship Program (to VL), US NSF grant 1536368 (to AC, DS, and SP), and the Tuttle Fund of the Department of Geosciences at Princeton University (to VL, DS).

Acknowledgments

We thank Kevin Wong and Rebecca Garley for collecting samples by scuba and the reviewers for improving the manuscript.

Conflict of interest

The authors declare that the research was conducted in the absence of any commercial or financial relationships that could be construed as a potential conflict of interest.

Generative AI statement

The author(s) declare that no Generative AI was used in the creation of this manuscript.

Publisher's note

References

Allemand, D., Tambutté, É., Girard, J. P., and Jaubert, J. (1998). Organic matrix synthesis in the scleractinian coral *Stylophora pistillata*: role in biomineralization and potential target of the organotin tributyltin. *J. Exp. Biol.* 201, 2001–2009. doi: 10.1242/jeb.201.13.2001

Altabet, M. A. (1988). Variations in nitrogen isotopic composition between sinking and suspended particles: Implications for nitrogen cycling and particle transformation in the open ocean. *Deep Sea Res. Part A Oceanogr. Res. Pap.* 35, 535–554. doi: 10.1016/0198-0149(88)90130-6

Anraku, M., and Omori, M. (1963). Preliminary survey of the relationship between the feeding habit and the structure of the mouth-parts of marine copepods. *Limnol. Oceanogr.* 8, 116–126. doi: 10.4319/lo.1963.8.1.0116

Badgley, B. D., Lipschultz, F., and Sebens, K. P. (2006). Nitrate uptake by the reef coral *Diploria 21trigose*: effects of concentration, water flow, and irradiance. *Mar. Biol.* 149, 327–338. doi: 10.1007/s00227-005-0180-5

Baker, D. M., Murdoch, T. J., Conti-Jerpe, I., and Fogel, M. (2017). Investigating Bermuda's pollution history through stable isotope analyses of modern and museum-

held gorgonian corals. *Mar. pollut. Bull.* 114, 169–175. doi: 10.1016/j.marpolbul.2016.08.069

Bermuda Ministry of Public Works (2023). *Sustainable water management for Bermuda's future*. Available online at: https://www.gov.bm/articles/sustainable-water-management-Bermuda%E2%80%99s-future (Accessed December 9, 2024).

Bouillon, S., Mohan, P. C., Sreenivas, N., and Dehairs, F. (2000). Sources of suspended organic matter and selective feeding by zooplankton in an estuarine mangrove ecosystem as traced by stable isotopes. *Mar. Ecol. Prog. Ser.* 208, 79–92. doi: 10.3354/meps208079

Braman, R. S., and Hendrix, S. A. (1989). Nanogram nitrite and nitrate determination in environmental and biological materials by vanadium (III) reduction with chemiluminescence detection. *Anal. Chem.* 61, 2715–2718. doi: 10.1021/ac00199a007

Brown, B. E., and Bythell, J. C. (2005). Perspectives on mucus secretion in reef corals. *Mar. Ecol. Prog. Ser.* 296, 291–309. doi: 10.3354/meps296291

Bythell, J. C. (1990). Nutrient uptake in the reef-building coral *Acropora palmata* at natural environmental concentrations. *Mar. Ecol. Prog. Ser.* 65, 65–69. doi: 10.3354/meps068065

Casciotti, K. L., Sigman, D. M., Hastings, M. G., Böhlke, J. K., and Hilkert, A. (2002). Measurement of the oxygen isotopic composition of nitrate in seawater and freshwater using the denitrifier method. *Anal. Chem.* 74, 4905–4912. doi: 10.1021/ac020113w

Choisnard, N., Duprey, N. N., Wald, T., Thibault, M., Houlbrèque, F., Foreman, A. D., et al. (2024). Tracing the fate of seabird-derived nitrogen in a coral reef using nitrate and coral skeleton nitrogen isotopes. *Limnol. Oceanogr.* 69, 309–324. doi: 10.1002/lno.12485

Conti-Jerpe, I. E., Thompson, P. D., Wong, C. W., Oliveira, N. L., Duprey, N. N., Moynihan, M. A., et al. (2020). Trophic strategy and bleaching resistance in reef-building corals. *Sci. Adv.* 6, eaaz5443. doi: 10.1126/sciadv.aaz5443

Corbett, D. R., Dillon, K., Burnett, W., and Schaefer, G. (2002). The spatial variability of nitrogen and phosphorus concentration in a sand aquifer influenced by onsite sewage treatment and disposal systems: a case study on St. George Island, Florida. *Environ. pollut.* 117, 337–345. doi: 10.1016/S0269-7491(01)00168-3

Corrège, T. (2006). Sea surface temperature and salinity reconstruction from coral geochemical tracers. *Palaeogeogr. Palaeoclimatol. Palaeoecol.* 232, 408–428. doi: 10.1016/j.palaeo.2005.10.014

Courtney, T. A., Lebrato, M., Bates, N. R., Collins, A., De Putron, S. J., Garley, R., et al. (2017). Environmental controls on modern scleractinian coral and reef-scale calcification. *Sci. Adv.* 3, e1701356. doi: 10.1126/sciadv.1701356

Davy, S. K., Allemand, D., and Weis, V. M. (2012). Cell biology of cnidarian-dinoflagellate symbiosis. *Microbiol. Mol. Biol. Rev.* 76, 229–261. doi: 10.1128/mmbr.05014-11

DeCarlo, T. M., Ren, H., and Farfan, G. A. (2018). The origin and role of organic matrix in coral calcification: insights from comparing coral skeleton and abiogenic aragonite. *Front. Mar. Sci.* 5. doi: 10.3389/fmars.2018.00170

DeMott, W. R. (1988). Discrimination between algae and detritus by freshwater and marine zooplankton. *Bull. Mar. Sci.* 43, 486–499.

DeMott, W. R. (1995). Optimal foraging by a suspension-feeding copepod: responses to short-term and seasonal variation in food resources. *Oecologia* 103, 230–240. doi: 10.1007/bf00329085

DeNiro, M. J., and Epstein, S. (1981). Influence of diet on the distribution of nitrogen isotopes in animals. *Geochim. Cosmochim. Acta* 45, 341–351. doi: 10.1016/0016-7037(81)90244-1

Devlin, Q. B. (2015). Nutrient dynamics in the coral-algal symbiosis: Developing insight from biogeochemical techniques. *Univ. Miami Miami*.

Drake, J. L., Mass, T., Haramaty, L., Zelzion, E., Bhattacharya, D., and Falkowski, P. G. (2013). Proteomic analysis of skeletal organic matrix from the stony coral *Stylophora pistillata*. *Proc. Natl. Acad. Sci. U.S.A.* 110, 3788–3793. doi: 10.1073/pnas.1301419110

Druffel, E. R. (1997). Geochemistry of corals: Proxies of past ocean chemistry, ocean circulation, and climate. *Proc. Natl. Acad. Sci. U.S.A.* 94, 8354–8361. doi: 10.1073/pnas.94.16.8354

Duprey, N. N., Wang, T. X., Kim, T., Cybulski, J. D., Vonhof, H. B., Crutzen, P. J., et al. (2020). Megacity development and the demise of coastal coral communities: Evidence from coral skeleton δ^{15}N records in the Pearl River estuary. *Glob. Chang. Biol.* 26, 1338–1353. doi: 10.1111/gcb.14923

Duprey, N. N., Wang, X. T., Thompson, P. D., Pleadwell, J. E., Raymundo, L. J., Kim, K., et al. (2017). Life and death of a sewage treatment plant recorded in a coral skeleton δ^{15}N record. *Mar. pollut. Bull.* 120, 109–116. doi: 10.1016/j.marpolbul.2017.04.023

Erler, D. V., Dudgeon, C. L., Armstrong, A. O., Banks, E. W., Ramirez-Valle, O., Gutiérrez-Jurado, H. A., et al. (2024). Linking transpiration to reef nitrogen supply on a tropical coral island. *J. Geophys. Res. Biogeosci.* 129, e2023JG007413. doi: 10.1029/2023JG007413

Erler, D. V., Farid, H. T., Glaze, T. D., Carlson-Perret, N. L., and Lough, J. M. (2020). Coral skeletons reveal the history of nitrogen cycling in the coastal Great Barrier Reef. *Nat. Commun.* 11, 1500. doi: 10.1038/s41467-020-15278-w

Erler, D. V., Nothdurft, L., McNeil, M., and Moras, C. A. (2018). Tracing nitrate sources using the isotopic composition of skeletal-bound organic matter from the calcareous green algae. *Halimeda. Coral Reefs* 37, 1003–1011. doi: 10.1007/s00338-018-1795-5

Erler, D. V., Wang, X. T., Sigman, D. M., Scheffers, S. R., Martínez-García, A., and Haug, G. H. (2016). Nitrogen isotopic composition of organic matter from a 168 year-old coral skeleton: Implications for coastal nutrient cycling in the Great Barrier Reef Lagoon. *Earth Planet Sci. Lett.* 434, 161–170. doi: 10.1016/j.epsl.2016.03.012

Erler, D. V., Wang, X. T., Sigman, D. M., Scheffers, S. R., and Shepherd, B. O. (2015). Controls on the nitrogen isotopic composition of shallow water corals across a tropical reef flat transect. *Coral Reefs* 34, 329–338. doi: 10.1007/s00338-014-1215-5

Falini, G., Fermani, S., and Goffredo, S. (2015). Coral biomineralization: A focus on intra-skeletal organic matrix and calcification. *Semin. Cell Dev. Biol.* 46, 17–26. doi: 10.1016/j.semcdb.2015.09.005

Fauchald, K., and Jumars, P. A. (1979). The diet of worms: A study of polychaete feeding guilds. *Oceanogr. Mar. Biol. Annu. Rev.* 17, 193–284.

Fawcett, S. E., Ward, B. B., Lomas, M. W., and Sigman, D. M. (2015). Vertical decoupling of nitrate assimilation and nitrification in the Sargasso Sea. *Deep Sea Res. I* 103, 64–72. doi: 10.1016/j.dsr.2015.05.004

Ferrier-Pagès, C., Rottier, C., Beraud, E., and Levy, O. (2010). Experimental assessment of the feeding effort of three scleractinian coral species during thermal stress: Effect on the rates of photosynthesis. *J. Exp. Mar. Biol. Ecol.* 390, 118–124. doi: 10.1016/j.jembe.2010.05.007

Ferrier-Pagès, C., Witting, J., Tambutté, E., and Sebens, K. P. (2003). Effect of natural zooplankton feeding on the tissue and skeletal growth of the scleractinian coral *Stylophora pistillata*. *Coral Reefs* 22, 229–240. doi: 10.1007/s00338-003-0312-7

Fujii, T., Tanaka, Y., Maki, K., Saotome, N., Morimoto, N., Watanabe, A., et al. (2020). Organic carbon and nitrogen isoscapes of reef corals and algal symbionts: Relative influences of environmental gradients and heterotrophy. *Microorganisms* 8 (8), 1221. doi: 10.3390/microorganisms8081221

Genin, A., Jaffe, J. S., Reef, R., Richter, C., and Franks, P. J. (2005). Swimming against the flow: A mechanism of zooplankton aggregation. *Science* 308, 860–862. doi: 10.1126/science.110783

Goreau, T. F. (1959). The ecology of Jamaican coral reefs I. Species composition and zonation. *Ecology* 40, 67–90. doi: 10.2307/1929924

Goreau, T. F., Goreau, N. I., and Yonge, C. M. (1971). Reef corals: Autotrophs or heterotrophs? *Biol. Bull.* 141, 247–260. doi: 10.2307/1540115

Granger, J., and Mathuri, M. (2021). *Nitrogen isotope fractionation for ammonium assimilation by marine phytoplankton (Biological Nitrogen Isotope Fractionation Project)* (BCO-DMO). Available at: http://lod.bco-dmo.org/id/dataset/864826 (Accessed March 9, 2025).

Grover, R., Maguer, J. F., Allemand, D., and Ferrier-Pagès, C. (2003). Nitrate uptake in the scleractinian coral *Stylophora pistillata*. *Limnol. Oceanogr.* 48, 2266–2274. doi: 10.4319/lo.2003.48.6.2266

Grover, R., Maguer, J. F., Allemand, D., and Ferrier-Pages, C. (2006). Urea uptake by the scleractinian coral Stylophora pistillata. *J. Exp. Mar. Biol. Ecol.* 332, 216–225. doi: 10.1016/j.jembe.2005.11.020

Grover, R., Maguer, J. F., Allemand, D., and Ferrier-Pages, C. (2008). Uptake of dissolved free amino acids by the scleractinian coral Stylophora pistillata. *J. Exp. Biol.* 211, 860–865. doi: 10.1242/jeb.01280

Grover, R., Maguer, J. F., Reynaud-Vaganay, S., and Ferrier-Pagès, C. (2002). Uptake of ammonium by the scleractinian coral *Stylophora pistillata*: Effect of feeding, light, and ammonium concentrations. *Limnol. Oceanogr.* 47, 782–790. doi: 10.4319/lo.2002.47.3.0782

Gustafsson, M. S., Baird, M. E., and Ralph, P. J. (2013). The interchangeability of autotrophic and heterotrophic nitrogen sources in Scleractinian coral symbiotic relationships: A numerical study. *Ecol. Model.* 250, 183–194. doi: 10.1016/j.ecolmodel.2012.11.003

Hoegh-Gulberg, O. (2004). Coral reefs in a century of rapid environmental change. *Symbiosis* 37, 1–31.

Hoegh-Guldberg, O., and Williamson, J. (1999). Availability of two forms of dissolved nitrogen to the coral *Pocillopora damicornis* and its symbiotic zooxanthellae. *Mar. Biol.* 133, 561–570. doi: 10.1007/s002270050496

Holmes, R. M., Aminot, A., Kérouel, R., Hooker, B. A., and Peterson, B. J. (1999). A simple and precise method for measuring ammonium in marine and freshwater ecosystems. *Can. J. Fish Aquat. Sci.* 56, 1801–1808. doi: 10.1139/f99-128

Houlbrèque, F., and Ferrier-Pagès, C. (2009). Heterotrophy in tropical scleractinian corals. *Biol. Rev.* 84, 1–17. doi: 10.1111/j.1469-185X.2008.00058.x

Houlbrèque, F., Tambutté, E., Allemand, D., and Ferrier-Pagès, C. (2004). Interactions between zooplankton feeding, photosynthesis and skeletal growth in the scleractinian coral *Stylophora pistillata*. *J. Exp. Biol.* 207, 1461–1469. doi: 10.1242/jeb.00911

Ingalls, A. E., Lee, C., and Druffel, E. R. (2003). Preservation of organic matter in mound-forming coral skeletons. *Geochim. Cosmochim. Acta* 67, 2827–2841. doi: 10.1016/S0016-7037(03)00079-6

Inoue, M., Nakamura, T., Tanaka, Y., Suzuki, A., Yokoyama, Y., Kawahata, H., et al. (2018). A simple role of coral-algal symbiosis in coral calcification based on multiple geochemical tracers. *Geochim. Cosmochim. Acta* 235, 76–88. doi: 10.1016/j.gca.2018.05.016

Jones, R., Parsons, R., Watkinson, E., and Kendell, D. (2011). Sewage contamination of a densely populated coral 'atoll'(Bermuda). *Environ. Monit. Assess.* 179, 309–324. doi: 10.1007/s10661-010-1738-3

Jørgensen, C. B. (1996). Bivalve filter feeding revisited. *Mar. Ecol. Prog. Ser.* 142, 287–302. doi: 10.3354/meps142287

Kaandorp, J. A., Sloot, P. M., Merks, R. M., Bak, R. P., Vermeij, M. J., and Maier, C. (2005). Morphogenesis of the branching reef coral *Madracis mirabilis*. *Proc. R Soc. B* 272, 127–133. doi: 10.1098/rspb.2004.2934

Kopp, C., Pernice, M., Domart-Coulon, I., Djediat, C., Spangenberg, J. E., Alexander, D. T., et al. (2013). Highly dynamic cellular-level response of symbiotic coral to a sudden increase in environmental nitrogen. *Mbio* 4, e01012–e01013. doi: 10.1128/mbio.00052-13

Lewis, J. B., and Price, W. S. (1975). Feeding mechanisms and feeding strategies of Atlantic reef corals. *J. Zool.* 176, 527–544. doi: 10.1111/j.1469-7998.1975.tb03219.x

Lonsdale, D. J., Heinle, D. R., and Siegfried, C. (1979). Carnivorous feeding behavior of the adult calanoid copepod *Acartia tonsa* Dana. *J. Exp. Mar. Biol. Ecol.* 36, 235–248. doi: 10.1016/0022-0981(79)90119-9

Marion, G. S., Dunbar, R. B., Mucciarone, D. A., Kremer, J. N., Lansing, J. S., and Arthawiguna, A. (2005). Coral skeletal $\delta^{15}N$ reveals isotopic traces of an agricultural revolution. *Mar. pollut. Bull.* 50, 931–944. doi: 10.1016/j.marpolbul.2005.04.001

Martinez, S., Grover, R., Baker, D. M., and Ferrier-Pages, C. (2022). Symbiodiniaceae are the first site of heterotrophic nitrogen assimilation in reef-building corals. *mBio* 13, e0160122. doi: 10.1128/mbio.01601-22

Marubini, F., and Davies, P. S. (1996). Nitrate increases zooxanthellae population density and reduces skeletogenesis in corals. *Mar. Biol.* 127, 319–328. doi: 10.1007/BF00942117

Mass, T., Putnam, H. M., Drake, J. L., Zelzion, E., Gates, R. D., Bhattacharya, D., et al. (2016). Temporal and spatial expression patterns of biomineralization proteins during early development in the stony coral *Pocillopora damicornis*. *Proc. R Soc. B* 283, 20160322. doi: 10.1098/rspb.2016.0322

McIlvin, M. R., and Casciotti, K. L. (2011). Technical updates to the bacterial method for nitrate isotopic analyses. *Anal. Chem.* 83, 1850–1856. doi: 10.1021/ac1028984

Mills, M. M. (2000). *Corals feeding on sediments? Ingestion, assimilation, and contributions to coral nutrition* (College Park, MD: University of Maryland, College Park).

Mills, M. M., Lipschultz, F., and Sebens, K. P. (2004). Particulate matter ingestion and associated nitrogen uptake by four species of scleractinian corals. *Coral Reefs* 23, 311–323. doi: 10.1007/s00338-004-0380-3

Minagawa, M., and Wada, E. (1984). Stepwise enrichment of ^{15}N along food chains: further evidence and the relation between $\delta^{15}N$ and animal age. *Geochim. Cosmochim. Acta* 48, 1135–1140. doi: 10.1016/0016-7037(84)90204-7

Muscatine, L., and D'Elia, C. F. (1978). The uptake, retention, and release of ammonium by reef corals. *Limnol. Oceanogr.* 23, 725–734. doi: 10.4319/lo.1978.23.4.0725

Muscatine, L., Porter, J. W., and Kaplan, I. R. (1989). Resource partitioning by reef corals as from stable isotope composition, I: d13C of zooxanthellae and animal tissue vs depth. *Mar Biol* 100, 185–193. doi: 10.1007/BF00391957

Muscatine, L., Goiran, C., Land, L., Jaubert, J., Cuif, J. P., and Allemand, D. (2005). Stable isotopes ($\delta^{13}C$ and $\delta^{15}N$) of organic matrix from coral skeleton. *Proc. Natl. Acad. Sci. U.S.A.* 102, 1525–1530. doi: 10.1073/pnas.0408921102

Nielsen, J. M., Popp, B. N., and Winder, M. (2015). Meta-analysis of amino acid stable nitrogen isotope ratios for estimating trophic position in marine organisms. *Oecologia* 178, 631–642. doi: 10.1007/s00442-015-3305-7

O'Connell, T. (2017). [amp]]lsquo;Trophic' and 'source' amino acids in trophic estimation: a likely metabolic explanation. *Oecologia* 184, 317–326. doi: 10.1007/s00442-017-3881-9

Palardy, J. E., Grottoli, A. G., and Matthews, K. A. (2006). Effect of naturally changing zooplankton concentrations on feeding rates of two coral species in the Eastern Pacific. *J. Exp. Mar. Biol. Ecol.* 331, 99–107. doi: 10.1016/j.jembe.2005.10.001

Pennock, J. R., Velinsky, D. J., Sharp, J. H., Ludlam, J., and Fogel, M. L. (1996). Isotope fractionation of ammonium and nitrate during their uptake by *Skeletonema costatum*: Implications for the $\delta^{15}N$ dynamics under bloom conditions. *Limnol. Oceanogr.* 41, 451–459. doi: 10.4319/lo.1996.41.3.0451

Pernice, M., Meibom, A., Van Den Heuvel, A., Kopp, C., Domart-Coulon, I., Hoegh-Guldberg, O., et al. (2012). A single-cell view of ammonium assimilation in coral–dinoflagellate symbiosis. *ISME J.* 6, 1314–1324. doi: 10.1038/ismej.2011.196

Piper, R. (2007). *Extraordinary animals: An encyclopedia of curious and unusual animals* (Greenwood Press, Westport, CT: Bloomsbury Publishing USA).

Plummer, L. N., Vacher, H. L., Mackenzie, F. T., Bricker, O. P., and Land, L. S. (1976). Hydrogeochemistry of Bermuda: A case history of ground-water diagenesis of biocalcarenites. *Geol. Soc. Am. Bull.* 87, 1301–1316. doi: 10.1130/0016-7606(1976)87<1301:HOBACH>2.0.CO;2

Popp, B. N., Graham, B. S., Olson, R. J., Hannides, C. C., Lott, M. J., López-Ibarra, G. A., et al. (2007). Insight into the trophic ecology of yellowfin tuna, *Thunnus albacares*, from compound-specific nitrogen isotope analysis of proteinaceous amino acids. *Terrestrial Ecol.* 1, 173–190. doi: 10.1016/S1936-7961(07)01012-3

Post, D. M. (2002). Using stable isotopes to estimate trophic position: models, methods, and assumptions. *Ecology* 83, 703–718. doi: 10.1890/0012-9658(2002)083[0703:USITET]2.0.CO;2

Puverel, S., Tambutté, E., Pereira-Mouries, L., Zoccola, D., Allemand, D., and Tambutté, S. (2005). Soluble organic matrix of two Scleractinian corals: partial and comparative analysis. *Comp. Biochem. Physiol. B Biochem. Mol. Biol.* 141, 480–487. doi: 10.1016/j.cbpc.2005.05.013

Rangel, M. S., Erler, D., Tagliafico, A., Cowden, K., Scheffers, S., and Christidis, L. (2019). Quantifying the transfer of prey $\delta^{15}N$ signatures into coral holobiont nitrogen pools. *Mar. Ecol. Prog. Ser.* 610, 33–49. doi: 10.3354/meps12847

Ren, H., Chen, Y. C., Wang, X. T., Wong, G. T., Cohen, A. L., DeCarlo, T. M., et al. (2017). 21st-century rise in anthropogenic nitrogen deposition on a remote coral reef. *Science* 356, 749–752. doi: 10.1126/science.aal3869

Richman, S., Heinle, D. R., and Huff, R. (1977). Grazing by adult estuarine calanoid copepods of the Chesapeake Bay. *Mar. Biol.* 42, 69–84. doi: 10.1007/BF00392015

Rowe, M. (1984). The freshwater "central lens" of Bermuda. *J. Hydrol* 73, 165–176. doi: 10.1016/0022-1694(84)90038-6

Schmitt, F. G., and Seuront, L. (2001). Multifractal random walk in copepod behavior. *Physica A* 301, 375–396. doi: 10.1016/S0378-4371(01)00429-0

Sebens, K. P., Grace, S. P., Helmuth, B., Maney, E. J. Jr, and Miles, J. S. (1998). Water flow and prey capture by three scleractinian corals, *Madracis mirabilis*, *Montastrea cavernosa*, and *Porites porites*, in a field enclosure. *Mar. Biol.* 131, 347–360. doi: 10.1007/S002270050328

Seuront, L., Yamazaki, H., and Souissi, S. (2004). Hydrodynamic disturbance and zooplankton swimming behavior. *Zool. Stud.* 43, 376–387.

Sigman, D. M., Casciotti, K. L., Andreani, M., Barford, C., Galanter, M. B. J. K., and Böhlke, J. K. (2001). A bacterial method for the nitrogen isotopic analysis of nitrate in seawater and freshwater. *Anal. Chem.* 73, 4145–4153. doi: 10.1021/ac010088e

Simmons, J. A. K. (1983). The biogeochemistry of the Devonshire lens, Bermuda. M.S. thesis. University of New Hampshire, Durham.

Simmons, J. K., Jickells, T., Knap, A., and Lyons, W. B. (1985). Nutrient concentrations in groundwaters from Bermuda: Anthropogenic effects, 383–398. In D. E. Caldwell and J. A. Brierly (eds.), *Planetary Ecol.* Van Nostrand Reinhold Company, Inc., New York.

Simmons, J. K., and Lyons, W. B. (1994). The ground water flux of nitrogen and phosphorus to Bermuda's coastal waters. *JAWRA J. Am. Water Resour. Assoc.* 30, 983–991. doi: 10.1111/j.1752-1688.1994.tb03346.x

Sims, Z. C., Cohen, A. L., Luu, V. H., Wang, X. T., and Sigman, D. M. (2020). Uptake of groundwater nitrogen by a near-shore coral reef community on Bermuda. *Coral Reefs* 39, 215–228. doi: 10.1007/s00338-019-01879-5

Stanley, G. D. Jr. (1981). Early history of scleractinian corals and its geological consequences. *Geology* 9, 507–511. doi: 10.1130/0091-7613(1981)9<507:EHOSCA>2.0.CO;2

Swart, P. K., Evans, S., Capo, T., and Altabet, M. A. (2014). The fractionation of nitrogen and oxygen isotopes in macroalgae during the assimilation of nitrate. *Biogeosciences* 11, 6147–6157. doi: 10.5194/bg-11-6147-2014

Szmant-Froelich, A., and Pilson, M. E. Q. (1984). Effects of feeding frequency and symbiosis with zooxanthellae on nitrogen metabolism and respiration of the coral *Astrangia danae*. *Mar. Biol.* 81, 153–162. doi: 10.1007/BF00393114

Tambutté, S., Holcomb, M., Ferrier-Pagès, C., Reynaud, S., Tambutté, É., Zoccola, D., et al. (2011). Coral biomineralization: From the gene to the environment. *J. Exp. Mar. Biol. Ecol.* 408, 58–78. doi: 10.1016/j.jembe.2011.07.026

Tanaka, Y., Miyajima, T., Koike, I., Hayashibara, T., and Ogawa, H. (2006). Translocation and conservation of organic nitrogen within the coral-zooxanthella symbiotic system of *Acropora pulchra*, as demonstrated by dual isotope-labeling techniques. *J. Exp. Mar. Biol. Ecol.* 336, 110–119. doi: 10.1016/j.jembe.2006.04.011

Tanaka, Y., Suzuki, A., and Sakai, K. (2018). The stoichiometry of coral-dinoflagellate symbiosis: carbon and nitrogen cycles are balanced in the recycling and double translocation system. *ISME J.* 12, 860–868. doi: 10.1038/s41396-017-0019-3

Thibault, M., Houlbreque, F., Duprey, N. N., Choisnard, N., Gillikin, D. P., Meunier, V., et al. (2022). Seabird-derived nutrients supply modulates the trophic strategies of mixotrophic corals. *Front. Mar. Sci.* 8. doi: 10.3389/fmars.2021.790408

Vacher, H. L. (1974). *Groundwater hydrology of Bermuda* (Bermuda: Public Works Department).

Vacher, H. L. (1978). Hydrogeology of Bermuda—Significance of an across-the-island variation in permeability. *J. Hydrol* 39, 207–226. doi: 10.1016/0022-1694(78)90001-X

Visser, A. W. (2007). Motility of zooplankton: fitness, foraging and predation. *J. Plankton Res.* 29, 447–461. doi: 10.1093/plankt/fbm029

Wang, X. T., Cohen, A. L., Luu, V., Ren, H., Su, Z., Haug, G. H., et al. (2018). Natural forcing of the North Atlantic nitrogen cycle in the Anthropocene. *Proc. Natl. Acad. Sci. U.S.A.* 115, 10606–10611. doi: 10.1073/pnas.180104911

Wang, X. T., Sigman, D. M., Cohen, A. L., Sinclair, D. J., Sherrell, R. M., Cobb, K. M., et al. (2016). Influence of open ocean nitrogen supply on the skeletal $\delta^{15}N$ of modern shallow-water scleractinian corals. *Earth Planet Sci. Lett.* 441, 125–132. doi: 10.1016/j.epsl.2016.02.032

Wang, X. T., Sigman, D. M., Cohen, A. L., Sinclair, D. J., Sherrell, R. M., Weigand, M. A., et al. (2015). Isotopic composition of skeleton-bound organic nitrogen in reef-building symbiotic corals: A new method and proxy evaluation at Bermuda. *Geochim. Cosmochim. Acta* 148, 179–190. doi: 10.1016/j.gca.2014.09.017

Waser, N., Harrison, P. J., Nielsen, B., and Calvert, S. E. (1998). Nitrogen isotope fractionation during the uptake and assimilation of nitrate, nitrite, ammonium, and urea by a marine diatom. *Limnol. Oceanogr.* 43, 215–224. doi: 10.4319/lo.1998.43.2.0215

Webb, K. L., and Wiebe, W. J. (1978). The kinetics and possible significance of nitrate uptake by several algal-invertebrate symbioses. *Mar. Biol.* 47, 21–27. doi: 10.1007/BF00397015

Weigand, M. A., Foriel, J., Barnett, B., Oleynik, S., and Sigman, D. M. (2016). Updates to instrumentation and protocols for isotopic analysis of nitrate by the denitrifier method. *Rapid Commun. Mass Spectrom.* 30, 1365–1383. doi: 10.1002/rcm.7570

Wiedenmann, J., D'Angelo, C., Mardones, M. L., Moore, S., Benkwitt, C. E., Graham, N. A., et al. (2023). Reef-building corals farm and feed on their photosynthetic symbionts. *Nature* 620, 1018–1024. doi: 10.1038/s41586-023-06442-5

Wilkerson, F. P., and Trench, R. K. (1986). Uptake of dissolved inorganic nitrogen by the symbiotic clam *Tridacna gigas* and the coral *Acropora* sp. *Mar. Biol.* 93, 237–246. doi: 10.1007/BF00508261

Yamazaki, H., and Squires, K. D. (1996). Comparison of oceanic turbulence and copepod swimming. *Mar. Ecol. Prog. Ser.* 144, 299–301. doi: 10.3354/meps144299

Yamazaki, A., Watanabe, T., Ogawa, N. O., Ohkouchi, N., Shirai, K., Toratani, M., et al. (2011b). Seasonal variations in the nitrogen isotope composition of Okinotori coral in the tropical western Pacific: A new proxy for marine nitrate dynamics. *J. Geophys. Res. Biogeosci.* 116, G4. doi: 10.1029/2011JG001697

Yamazaki, A., Watanabe, T., and Tsunogai, U. (2011a). Nitrogen isotopes of organic nitrogen in reef coral skeletons as a proxy of tropical nutrient dynamics. *Geophys. Res. Lett.* 38, 19. doi: 10.1029/2011GL049053

Young, S. D., O'Connor, J. D., and Muscatine, L. (1971). Organic material from scleractinian coral skeletons—II. Incorporation of ^{14}C into protein, chitin and lipid. *Comp. Biochem. Physiol. B Comp. Biochem.* 40, 945–958. doi: 10.1016/0305-0491(71)90040-X

Zaquin, T., Malik, A., Drake, J. L., Putnam, H. M., and Mass, T. (2021). Evolution of protein-mediated biomineralization in scleractinian corals. *Front. Genet.* 12. doi: 10.3389/fgene.2021.618517